ACKNOWLEDGMENTS

We thank B. de Crombrugghe for the *Col1a1* promoter, L. Bonewald for MLO-A5, Y. Ito for Runx2 antibody, Yamanouchi Pharmaceutical Co. Ltd for rhBMP-2, F. Ikeda and H. Murayama for technical advice, K. Nonaka (Elk Corporation) for performing pQCT analysis, N. Komatsu and K. Kawagoe for maintaining mouse colonies, and A. Kakiya for secretarial assistance.

REFERENCES

Ducy P, Zhang R, Geoffroy V, Ridall AL, Karsenty G. 1997. Osf2/Cbfa1: a transcriptional activator of osteoblast differentiation. Cell 89:747–754.

Ducy P, Starbuck M, Priemel M, Shen J, Pinero G, Geoffroy V, Amling M, Karsenty G. 1999. A Cbfa1-dependent genetic pathway controls bone formation beyond embryonic development. Genes Dev 13:1025–1036.

Enomoto H, Shiojiri S, Hoshi K, Furuichi T, Fukuyama R, Yoshida C, Kanatani N, Nakamura R, Mizuno A, Zanma A, Yano K, Yasuda H, Higashio K, Takada K, Komori T. 2003. Induction of osteoclast differentiation by Runx2 through RANKL and OPG regulation and partial rescue of osteoclastogenesis in Runx2$^{-/-}$ mice by RANKL transgene. J Biol Chem 278: 23971–23977.

Enomoto H, Furuichi T, Zanma A, Yamana K, Yoshida C, Sumitani S, Yamamoto H, Enomoto-Iwamoto M, Iwamoto M, Komori T. 2004. Runx2 deficiency in chondrocytes causes adipogenic changes in vitro. J Cell Sci 117:417–425.

Frolik CA, Black EC, Cain RL, Satterwhite JH, Brown-Augsburger PL, Sato M, Hock JM. 2003. Anabolic and catabolic bone effects of human parathyroid hormone (1-34) are predicted by duration of hormone exposure. Bone. 33:372–379.

Geoffroy V, Kneissel M, Fournier B, Boyde A, and Matthias P. 2002. High bone resorption in adult aging transgenic mice overexpressing cbfa1/runx2 in cells of the osteoblastic lineage. Mol Cell Biol 22:6222–6233.

Harada H, Tagashira S, Fujiwara M, Ogawa S, Katsumata T, Yamaguchi A, Komori T, and Nakatsuka M. 1999. Cbfa1 isoforms exert functional differences in osteoblast differentiation. J Biol Chem 274:6972–6978.

Inada M, Yasui T, Nomura S, Miyake S, Deguchi K, Himeno M, Sato M, Yamagiwa H, Kimura T, Yasui N, Ochi T, Endo N, Kitamura Y, Kishimoto T, Komori T. 1999. Maturational disturbance of chondrocytes in Cbfa1-deficient mice. Dev Dyn 214:279–290.

Javed A, Gutierrez S, Montecino M, van Wijnen AJ, Stein JL, Stein GS, Lian JB. 1999. Multiple Cbfa/AML sites in the rat osteocalcin promoter are required for basal and vitamin D-responsive transcription and contribute to chromatin organization. Mol Cell Biol 19:7491–7500.

Kanatani N, Fujita T, Fukuyama R, Liu W, Yoshida CA, Moriishi T, Yamana K, Miyazaki T, Toyosawa S, Komori T. 2006. Cbfβ regulates Runx2 function isoform-dependently in postnatal bone development. Dev Biol 296:48–61.

Kern B, Shen J, Starbuck M, Karsenty G. 2001. Cbfa1 contributes to the osteoblast-specific expression of type I collagen genes. J Biol Chem 276:7101–7107.

Komori T, Yagi H, Nomura S, Yamaguchi A, Sasaki K, Deguchi K, Shimizu Y, Bronson RT, Gao YH, Inada M, Sato M, Okamoto R, Kitamura Y, Yoshiki S, Kishimoto T. 1997. Targeted disruption of Cbfa1 results in a complete lack of bone formation owing to maturational arrest of osteoblasts. Cell 89:755–764.

Komori T. 2005. Regulation of skeletal development by the Runx family of transcription factors. J Cell Biochem 95:445–453.

Krishnan V, Moore TL, Ma YL, Helvering LM, Frolik CA, Valasek KM, Ducy P, Geiser AG. 2003. Parathyroid hormone bone anabolic action requires Cbfa1/Runx2 -dependent signaling. Mol Endocrinol 17:423–435.

Kundu M, Javed A, Jeon JP, Horner A, Shum L, Eckhaus M, Muenke M, Lian JB, Yang Y, Nuckolls GH, Stein GS, Liu PP. 2002. Cbfβ interacts with Runx2 and has a critical role in bone development. Nat Genet 32:639–644.

Liu W, Toyosawa S, Furuichi T, Kanatani N, Yoshida C, Liu Y, Himeno M, Narai S, Yamaguchi A, Komori T. 2001. Overexpression of Cbfa1 in osteoblasts inhibits osteoblast maturation and causes osteopenia with multiple fractures. J Cell Biol 155:157–166.

Manolagas SC, Jilka RL. 1995. Bone marrow, cytokines, and bone remodeling. Emerging insights into the pathophysiology of osteoporosis. N Engl J Med 332: 305–311.

Marks SC, Odgren PR. 2002. Structure and development of the skeleton. In: Bilezikian JP, Raisz LG, Rodan GA, editors. Principles of bone biology. London: Academic Press. p 3–15.

McCarthy TL, Chang WZ, Liu Y, Centrella M. 2003. Runx2 integrates estrogen activity in osteoblasts. J Biol Chem 278: 43121–43129.

Miller J, Horner A, Stacy T, Lowrey C, Lian JB, Stein G, Nuckolls GH, Speck NA. 2002. The core-binding factor β subunit is required for bone formation and hematopoietic maturation. Nat Genet 32: 645–649.

Otto F, Thornell AP, Crompton T, Denzel A, Gilmour KC, Rosewell IR, Stamp GW, Beddington RS, Mundlos S, Olsen BR, Selby PB, Owen MJ. 1997. Cbfa1, a candidate gene for cleidocranial dysplasia syndrome, is essential for osteoblast differentiation and bone development. Cell 89:765–771.

Pacifici R. 1996. Estrogen, cytokines, and pathogenesis of postmenopausal osteoporosis. J Bone Miner Res 11:1043–1051.

Rossert J, Eberspaecher H, de Crombrugghe B. 1995. Separate cis-acting DNA elements of the mouse pro-α1(I) collagenpromoter direct expression of reporter genes to different type I collagen-producing cells in transgenic mice. J Cell Biol 129:1421–1432.

Sato M, Morii E, Komori T, Kawahata H, Sugimoto M, Terai K, Shimizu H, Yasui T, Ogihara H, Yasui N, Ochi T, Kitamura Y, Ito Y, Nomura S. 1998. Transcriptional regulation of osteopontin gene in vivo by PEBP2αA/CBFA1 and ETS1 in the skeletal tissues. Oncogene 17:1517–1525.

Ueta C, Iwamoto M, Kanatani N, Yoshida C, Liu Y, Enomoto-Iwamoto M, Ohmori T, Enomoto H, Nakata K, Takada K, Kurisu K, Komori T. 2001. Skeletal malformations caused by overexpression of Cbfa1 or its dominant-negative form in chondrocytes. J Cell Biol 153:87–99.

Xiao Z, Awad HA, Liu S, Mahlios J, Zhang S, Guilak F, Mayo MS, Quarles LD. 2005. Selective Runx2-II deficiency leads to low-turnover osteopenia in adult mice. Dev Biol 283:345–345.

Yoshida CA, Furuichi T, Fujita T, Fukuyama R, Kanatani N, Kobayashi S, Satake M, Takada K, Komori T. 2002. Core-binding factor β interacts with Runx2 and is required for skeletal development. Nat Genet 32:633–638.

Zelzer E, Glotzer DJ, Hartmann C, Thomas D, Fukai N, Soker S, Olsen BR. 2001. Tissue specific regulation of VEGF expression during bone development requires Cbfa1/Runx2. Mech Dev 106:97–106.

THE JOURNAL OF BIOLOGICAL CHEMISTRY VOL. 282, NO. 28, pp. 20407–20415, July 13, 2007

Optimal Combination of Soluble Factors for Tissue Engineering of Permanent Cartilage from Cultured Human Chondrocytes*[S]

Received for publication, August 31, 2006, and in revised form, March 12, 2007 Published, JBC Papers in Press, May 10, 2007, DOI 10.1074/jbc.M608383200

Guangyao Liu[‡§], Hiroshi Kawaguchi[§], Toru Ogasawara[‡], Yukiyo Asawa[‡], Junji Kishimoto[¶], Tsuguharu Takahashi[‡], Ung-il Chung[‖], Hisayo Yamaoka[‡], Hirotaka Asato[§], Kozo Nakamura[§], Tsuyoshi Takato[§], and Kazuto Hoshi[‡1]

From the Departments of [‡]Cartilage and Bone Regeneration (Fujisoft), [§]Sensory and Motor System Medicine, and [¶]Clinical Bioinformatics, and [‖]Center of Disease Biology and Integrative Medicine, Faculty of Medicine, The University of Tokyo, Hongo 7-3-1, Bunkyo-ku, Tokyo 113-8655, Japan

Since permanent cartilage has poor self-regenerative capacity, its regeneration from autologous human chondrocytes using a tissue engineering technique may greatly benefit the treatment of various skeletal disorders. However, the conventional autologous chondrocyte implantation is insufficient both in quantity and in quality due to two major limitations: dedifferentiation during a long term culture for multiplication and hypertrophic differentiation by stimulation for the redifferentiation. To overcome the limitations, this study attempted to determine the optimal combination in primary human chondrocyte cultures under a serum-free condition, from among 12 putative chondrocyte regulators. From the exhaustive 2^{12} = 4,096 combinations, 256 were selected by fractional factorial design, and bone morphogenetic protein-2 and insulin (BI) were statistically determined to be the most effective combination causing redifferentiation of the dedifferentiated cells after repeated passaging. We further found that the addition of triiodothyronine (T3) prevented the BI-induced hypertrophic differentiation of redifferentiated chondrocytes via the suppression of Akt signaling. The implant formed by the human chondrocytes cultured in atelocollagen and poly(L-latic acid) scaffold under the BI + T3 stimulation consisted of sufficient hyaline cartilage with mechanical properties comparable with native cartilage after transplantation in nude mice, indicating that BI + T3 is the optimal combination to regenerate a clinically practical permanent cartilage from autologous chondrocytes.

Since cartilage has poor regenerative capacity by itself, its regeneration using a tissue engineering technique may greatly benefit the treatment of various skeletal disorders that cannot be treated by conventional methods. Although tissue-engineered cartilage from autologous chondrocytes is already available for clinical use (1–3), the size is less than 1 ml and is limited to just a filler of a small defect or an injectable plaque of the affected cartilage. To broaden its clinical indication to major disorders such as osteoarthritic joints, microtia, and cleft lip/palate, cartilaginous matrix should be abundantly produced by a sufficient number of autologous chondrocytes. Since the number of chondrocytes that can be isolated primarily from the native cartilage is limited, it should be markedly increased in culture. However, during their multiplication in culture through repeated passaging, chondrocytes inevitably lose their ability to produce cartilaginous matrix such as glycosaminoglycan (GAG)[2] and type II collagen (COL2) and begin producing type I collagen (COL1), which is called dedifferentiation (4). Although biochemical factors such as hormones and growth factors are known to stimulate redifferentiation of the dedifferentiated chondrocytes to restore the chondrocytic properties (5, 6), there remains another inevitable limitation, that is, induction of hypertrophic differentiation of chondrocytes (7), which leads to endochondral ossification as seen in the growth plates.

To develop a clinically practical tissue engineering of permanent cartilage that overcomes the limitations above, the present study focused on 12 representative soluble factors (8) that are known to be potent regulators of proliferation or differentiation of chondrocytes and have already been approved for safe clinical use. We initially determined a combination of two factors among them that most efficiently induce redifferentiation of the dedifferentiated human chondrocytes under a serum-free condition using a statistical method termed "analysis of variance by fractional factorial design" (9). We then selected a third factor that prevents the redifferentiated chondrocytes from hypertrophic differentiation and investigated the underlying

* This work was supported by Grants-in-Aid 15390539, 16390431, and 16659546 for Scientific Research from the Japanese Ministry of Education, Culture, Sports, Science and Technology, Daiwa Securities Health Foundation, and the Research Society for Metabolic Bone Diseases. The costs of publication of this article were defrayed in part by the payment of page charges. This article must therefore be hereby marked "*advertisement*" in accordance with 18 U.S.C. Section 1734 solely to indicate this fact.

[S] The on-line version of this article (available at http://www.jbc.org) contains supplemental figures.

[1] To whom correspondence should be addressed. Tel.: 81-3-5800-9891; Fax: 81-3-5800-9891; E-mail: pochi-tky@umin.net.

[2] The abbreviations used are: GAG, glycosaminoglycan; COL1, type I collagen; COL2, type II collagen; COL1A1, type I collagen α1 chain; COL2A1, type II collagen α1 chain; COL10A1, type X collagen α1 chain; FGF, fibroblast growth factor; BMP, bone morphogenetic protein; IGF, insulin-like growth factor; PTH, parathyroid hormone; PTH, PTH-related protein; IL-1RA, interleukin-1 receptor antagonist; T3, L-3,3′,5′-triiodothyronine; T4, L-thyroxin; MAPK, mitogen-activated protein kinase; PLLA, poly(L-lactic acid); BI, bone morphogenetic protein-2 and insulin; BIT, BI and T3; RT, reverse transcription; TUNEL, terminal deoxynucleotidyltransferase-mediated dUTP nick end-labeling; TRα, thyroid hormone receptor-α; rh, recombinant human.

molecular mechanism. Finally, we evaluated the properties of the tissue-engineered cartilage by the selected combination to examine whether it is applicable to clinical use for the treatment of major skeletal disorders.

EXPERIMENTAL PROCEDURES

Cell Isolation and Monolayer Culture—All procedures of the present experiments were approved by the ethics committee of the University of Tokyo Hospital (ethics permission number 622). Both remnant auricular cartilage and costal from one of six microtia patients (10–15 years old) were obtained during surgery in adherence to the Helsinki Principles. Chondrocytes were isolated with digestion using 0.15% collagenase (Wako Pure Chemical Industries, Osaka, Japan). Primary articular chondrocytes were purchased from Sanko Junyaku (Tokyo, Japan). The chondrocytes were seeded in a 100-mm plastic tissue culture dish at a density of 6,400 cells/cm^2 and cultured in Dulbecco's modified Eagle's medium/F12 containing 5% human serum supplemented with fibroblast growth factor-2 (FGF-2, 100 ng/ml) and insulin (5 μg/ml), as we reported previously (8). Passaging was performed by trypsin-EDTA solution (Sigma) and repeated until 1000-fold increase of the total cell number.

Generation of Cartilage Pellet and Implant—For three-dimensional atelocollagen culture, the dedifferentiated chondrocytes were suspended in 0.8% atelocollagen solution (Kawaken Fine Chemicals, Tokyo, Japan) at a density of 10^7 cells/ml. The atelocollagen pellets were cultured in Dulbecco's modified Eagle's medium/F-12 (Sigma) medium with or without soluble factors for 1–3 weeks. To make the cartilage implant, a 100 μl-atelocollagen aliquot containing 10^6 chondrocytes was added to a poly(L-latic acid) (PLLA) mesh (kindly provided by Unitika, Tokyo, Japan) (10). Animal experiments were performed according to the protocol approved by the Animal Care and Use Committee of the University of Tokyo.

Analysis of Variance by Fractional Factorial Design—We used recombinant human bone morphogenetic protein-2 (rhBMP-2, kindly provided by Astellas Pharma, Tokyo, Japan), rh-insulin (MP Biomedicals, Irvine, CA), rh-insulin-like growth factor-I (rhIGF-I, Former Genzyme-Techne, Minneapolis, MN), rh-testosterone (Ultrafine Chemicals, Manchester, UK), rh-parathyroid hormone (rhPTH (1-34), Anaspec, San Jose, CA), rh-interleukin-1 receptor antagonist (rhIL-1RA, Strathmann Biotech, Hamburg, Germany), rh-growth hormone (Biogenesis, Poole, UK), 17β-estradiol (EMD Bioscience, San Diego, CA), rh-L-3,3′,5′-triiodothyronine (rhT3, EMD Bioscience), 1α-25-dihydroxy vitamin D3 (EMD Bioscience), rhFGF-2 (kindly provided by Kaken Pharmaceutical Corp., Tokyo, Japan), and dexamethasone (EMD Bioscience). The dosage of each factor was determined to be: BMP-2, 200 ng/ml; insulin, 5 μg/ml; IGF-I, 100 ng/ml; testosterone, 1 μM; PTH, 5×10^{-8} M; IL-1RA, 20 ng/ml; growth hormone, 100 ng/ml; 17β-estradiol, 100 nM; T3, 100 nM; 1α-25-dihydroxy vitamin D3, 100 nM; FGF-2, 10 ng/ml; dexamethasone, 100 nM, based on previous reports by us and others (8, 11–20). These doses of individual factors were within the range between effective dose 75 and effective dose 100 of their proper effects on chondrocytes, according to dose-response curves in the previous reports (11, 12, 15, 16, 21–28).

The software JMP-5.1.1J (SAS Institute, Cary, NC) was used to choose 256 randomized combinations in which the 12 factors independently appeared in an incidence of 50%, from 2^{12} = 4,096 combinations (see the supplemental table). Auricular chondrocytes obtained from three different patients (5×10^4 cells in 5 μl of 0.8% atelocollagen gel) were cultured in Dulbecco's modified Eagle's medium/F-12 containing the combinations for 2 weeks, and the GAG accumulation was measured as described below. Parameter estimates of the GAG accumulation by one factor or two were calculated from the F values that represent the effects of the individual factors and the interaction terms of two factors by the analysis of variance using the software above.

Real-time RT-PCR Analysis—Total RNA was isolated from chondrocytes using the chaotropic TRIzol method (Nippongene, Tokyo, Japan). Total mRNA (1 μg) was reverse-transcribed using SuperScript reverse transcriptase with random hexamer (Takara Shuzo, Shiga, Japan). The full-length or partial-length cDNA of target genes, including PCR amplicon sequences, was amplified by PCR, cloned into pCR-TOPO Zero II or pCR-TOPO II vectors (Invitrogen), and used as standard templates after linearization. QuantiTect SYBR Green PCR Master Mix (Qiagen, Hilden, Germany) was used, and SYBR Green PCR amplification and real-time fluorescence detection were performed with an ABI 7700 sequence detection system (Foster City, CA). All reactions were run in quadruplicate. Sequences of primers were 5′-CTCCTCGCTTTCCTTCCTCT-3′ and 5′-GTGCTAAAGGTGCCAATGGT-3′ for type I collagen αI chain (COL1A1); 5′-GAGTCAAGGGTGATCGTGGT-3′ and 5′-CACCTTGGTCTCCAGAAGGA-3′ for type II collagen αI chain (COL2A1); 5′-AGGAATGCCTGTGTCTGCTT-3′ and 5′-ACAGGCCTACCCAAACATGA-3′ for type X collagen αI chain (COL10A1); 5′-CAGACCAGCAGCAGCCATA-3′ and 5′-CAGCGTCAACACCATCATTC-3′ for Runx2; 5′-CATGAGCGAGGGCACTCC-3′ and 5′-TCGCTTCAGGTCAGCCTTG-3′ for Sox9; 5′-ATGCAGCGGAGACTGGTTCAG-3′ and 5′-GTCCTTGGAAGGTCTCTGCTG-3′ for PTH/PTHrP receptor; 5′-GAAGGTGAAGGTCGGAGTCA-3′ and 5′-GAAGATGGTGATGGGATTTC-3′ for glyceraldehyde-3-phosphate dehydrogenase.

GAG Measurement—The sulfated GAG content was measured using Alcian blue binding assay (Wieslab AB, Lund, Sweden). After digestion of the atelocollagen pellet containing chondrocytes in 0.3% collagenase for 1 h at 37 °C, cell debris and insoluble material were removed by centrifugation at 6,000 × *g* for 30 min. GAG in the supernatant was precipitated with Alcian blue solution, and the sediments by centrifugation at 6,000 × *g* for 15 min were dissolved again in 4 M GuHCl-33% propanol solution. The spectrophotometrical absorbance of the mixture was measured at a wavelength of 600 nm.

Enzyme-linked Immunosorbent Assay for Type I and Type II Collagen—The collagen proteins of the pellets, the implants, and the native human auricular cartilage were quantified by enzyme-linked immunosorbent assay using a human Type 1 and Type 2 collagen detection kit (Chondrex, Redmond, WA). The pellets, the implants, or the native human auricular carti-

lage were dissolved in 10 mg/ml pepsin, 0.05 M acetic acid at 4 °C for 48 h and then in 1 mg/ml pancreatic elastase, 0.1 mM Tris, 0.02 M NaCl, 5 mM $CaCl_2$, (pH 7.8–8.0) at 4 °C overnight. The samples were centrifuged at 9,100 × *g* for 5 min to remove the residue. The collagen proteins were captured by polyclonal anti-human COL1 or COL2 antibodies and detected by biotinylated counterparts and streptavidin peroxidase. O-phenylenediamine and H_2O_2 were added to the mixture, and the spectrophotometrical absorbance of the mixture was measured at a wavelength of 490 nm.

Western Blot Analysis—Human auricular chondrocytes underwent three-dimensional atelocollagen culture with BI (BMP-2 (200 ng/ml) + insulin (5 μg/ml)) in the presence and absence of T3 (100 nM), an Akt inhibitor (1, 10, and 100 ng/ml, Akt inhibitor, 1L-6-hydroxymethyl-chiro-inositol 2-(*R*)-2-*O*-methyl-3-*O*-octadecylcarbonate, EMD Bioscience), or p38 mitogen-activated protein kinase (MAPK) inhibitor SB203580 (10 μM, Sigma) for 5, 10, or 30 min or 24 h. Samples were prepared using M-PER (Pierce Biotechnology) supplemented with Na_3VO_4 (2 mM), NaF (10 mM), and aprotinin (10 μg/ml). An equal amount (20 μg) of protein was subjected to SDS-PAGE and transferred onto polyvinylidene difluoride membranes. Rabbit polyclonal antibodies against Smad1/5/8, phospho-Smad1/5/8, p38 MAPK, phospho-p38 MAPK, Akt, phospho-Akt (all from Cell Signaling Technology, Beverly, MA), and actin (Sigma) were used as primary antibodies. The membrane was incubated with horseradish peroxidase-conjugated secondary antibody (Promega, Madison, MI). Immunoreactive proteins were visualized by ECL (Amersham Biosciences, Buckinghamshire, UK).

Histology, Histochemistry, and Fine Structure—The tissue-engineered cartilage was fixed with 4% paraformaldehyde, embedded in OCT compound (Sakura, Tokyo, Japan), and cryosectioned into 10-μm slices. The sections were stained with toluidine blue-O and TUNEL (ApopTag, Intergen, Purchase, NY) according to the manufacturer's instructions. For fluorescent immunohistochemistry, the sections were incubated with a mouse monoclonal anti-COL10 antibody (Sigma) and then with biotin-conjugated anti-mouse IgG + IgA + IgM antibodies (Nichirei, Tokyo, Japan) and fluorescein isothiocyanate-streptavidin. The localizations were observed by confocal laser scanning microscopy (Leica TCS-SL, Wetzler, Germany). For the ultrastructural observation, the specimens were immersed in a mixture of 2% paraformaldehyde and 2.5% glutaraldehyde. After postfixation with 1% OsO_4, the specimens were dehydrated in a graded ethanol series, replaced with propylene oxide, embedded in Poly/Bed 812 resin (Polysciences, Warrington, PA), and sliced into 60–80-nm sections. The sections were observed under a transmission electron microscope (Hitachi H-7100, Tokyo, Japan).

Mechanical Properties—Mechanical properties of the pellet and implant were measured using a Venustron tactile sensor (Axiom, Fukushima, Japan). With computer control, the motor-driven sensor unit automatically presses down the objects up to 0.5 mm in depth from the surface and provides the compression strength and the decrease in the resonant frequency. Young's modulus was calculated by the compression strength and the frequency decrease using the software Venus 42 (Axiom), based on a previous report (29).

Statistical Analysis—All data are expressed as means ± S.E. Means of groups were compared by analysis of variance, and significance of differences was determined by post hoc testing with Bonferroni's method.

RESULTS

Determination of the Optimal Combination of Soluble Factors—We attempted to determine the optimal combination of soluble factors for regeneration of permanent cartilage from cultured human chondrocytes that were isolated from remnant auricular cartilage of microtia patients during surgery. To gain a substantial number of cells, the chondrocytes were initially cultured in monolayer with repeated passaging until 1,000-fold increase of the total cell number as we previously reported (8), which took ~4 weeks. The dedifferentiated chondrocytes during the monolayer culture were further cultured in an atelocollagen gel in a three-dimensional condition under stimulation by combinations of 12 candidate factors, *i.e.* BMP-2, insulin, IGF-I, testosterone, PTH, IL-1RA, growth hormone, 17β-estradiol, T3, 1α-25-dihydroxy vitamin D3, FGF-2, and dexamethasone. The redifferentiation was determined by the GAG accumulation. Since exhaustive examination of $2^{12} = 4{,}096$ combinations was impossible, we adopted the fractional factorial design (9) for the faultless reduction of the experimental units to a practical number of 256 combinations (see the supplemental table). As a single factor, the statistical analysis revealed that BMP-2, insulin, and IGF-I were the most potent factors of the GAG accumulation (Fig. 1*A*). Regarding two factors, the combination of BMP-2 and insulin (BI) was shown to provide the most abundant GAG accumulation (Fig. 1*A*).

We then examined expressions of COL1A1, COL2A1, and COL10A1 by real-time RT-PCR in the cultured human auricular chondrocytes just after isolation (Fig. 1*B*, *primary*), after the monolayer culture (*pre-rediff*), and after the three-dimensional atelocollagen culture (Fig. 1*B*). The long term monolayer culture with repeated passaging led to an increase in COL1A1 and a decrease in COL2A1, confirming the dedifferentiation. The three-dimensional atelocollagen culture thereafter with no stimulation somewhat restored both COL1A1 and COL2A1 expressions, indicating redifferentiation, which was much more enhanced by the BI stimulation. However, BI also increased COL10A1, a marker of chondrocyte hypertrophic differentiation, which is a critical defect for the regeneration of permanent cartilage. Thus, we next searched among the other 10 factors for a third factor that not only enhances the COL1 inhibition and the COL2 stimulation by BI but also suppresses the COL10 induction and found that only T3 exhibited significant effects on all parameters. This indicates that T3 is the optimal third factor that enhances the advantage and cancels the disadvantage of BI for regeneration of permanent cartilage from human auricular chondrocytes.

When we used cultured chondrocytes from human articular cartilage (Fig. 1*C*) and human rib cartilage (Fig. 1*D*), the combination of BI and T3 (BIT) potently suppressed COL1A1 and COL10A1 and enhanced COL2A1 expressions,

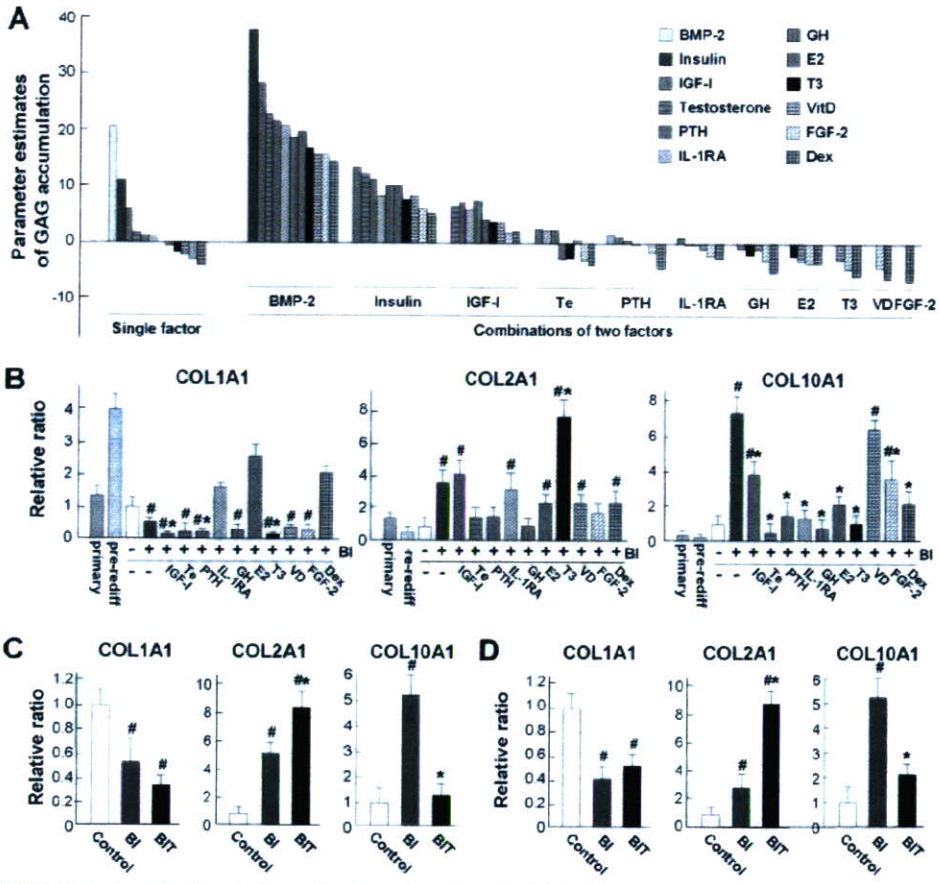

FIGURE 1. **Determination of the optimal combination of soluble factors.** *A*, parameter estimates of a single or two factors were statistically calculated from GAG accumulation in 256 combinations of 12 candidate factors. *GH*, growth hormone; *E2*, 17β-estradiol; *VitD*, 1α-25-dihydroxy vitamin D3; *Dex*, dexamethasone; *Te*, testosterone. *B*, COL1A1, COL2A1, and COL10A1 mRNA levels by real-time RT-PCR of the human auricular chondrocytes just after the isolation (*primary*), after the monolayer culture (*pre-rediff*), and after 1 week of the three-dimensional atelocollagen culture in the presence (+) and absence (−) of BMP-2 (200 ng/ml) + insulin (5 μg/ml) (BI) and a third factor from 10 other factors. *C* and *D*, COL1A1, COL2A1, and COL10A1 mRNA levels by real-time RT-PCR of cultured chondrocytes derived from human articular cartilage (*C*) and human rib cartilage (*D*). The dedifferentiated cells after multiplication in the monolayer culture underwent three-dimensional atelocollagen culture for 1 week in the presence and absence of BI or BI + T3 (100 nM) (BIT). For *B–D*, data are expressed as mean (*bars*) ± S.E. (*error bars*) of relative ratios of the control culture (−/−) for six cultures/group. #, $p < 0.01$, significant effects *versus* control; *, $p < 0.01$, significant effects by a third factor or T3 *versus* BI alone.

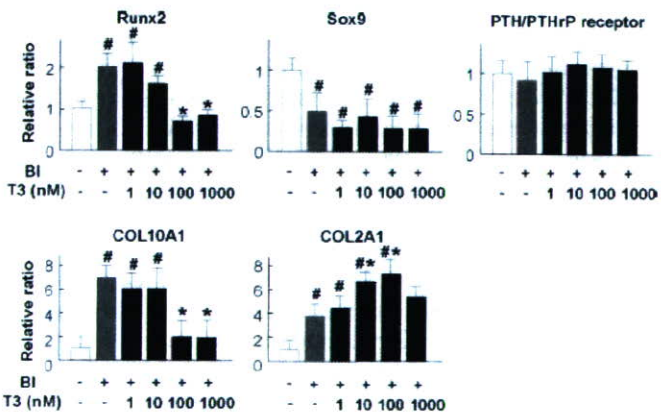

FIGURE 2. **Dose response effects of T3 (1–1000 nM) on mRNA levels of Runx2, Sox9, PTH/PTHrP receptor, COL10A1, and COL2A1 determined by real-time RT-PCR in three-dimensional atelocollagen culture.** The dedifferentiated chondrocytes after multiplication in the monolayer culture underwent the three-dimensional culture for 1 week under the stimulation. Data are expressed as mean (*bars*) ± S.E. (*error bars*) of relative ratios of the control culture for six cultures/group. BI, BMP-2 (200 ng/ml) + insulin (5 μg/ml). #, $p < 0.01$, significant effects *versus* control; *, $p < 0.01$, significant effects by T3 *versus* BI.

just as in the case of the human auricular cartilage. This indicates that BIT is universally efficacious for tissue engineering of permanent cartilage from human chondrocytes of various origins.

Mechanism Underlying the Preventive Effect of T3 on BI-induced Hypertrophic Differentiation of Redifferentiated Chondrocytes—To clarify the molecular mechanism whereby T3 prevented the BI-induced hypertrophic differentiation of redifferentiated chondrocytes, we examined the involvement of putative signalings that regulate hypertrophic differentiation in the three-dimensional atelocollagen culture of human auricular chondrocytes. Runx2, a member of the runt family of transcription factors, is known to be required for chondrocyte hypertrophy (30). Sox9, an essential factor for chondrogenic differentiation (31), functions as a potent inhibitor of chondrocyte hypertrophy (32). PTH/PTHrP via the cAMP-dependent protein kinase is also known to be a major factor that inhibits chondrocyte hypertrophy (33). Among the three factors above, T3 dose-dependently suppressed the BI stimulation of expression of Runx2 similarly to that of COL10A1, but not that of Sox9 or PTH/PTHrP receptor, implying that Runx2 is involved in the prevention of the BI-induced hypertrophic differentiation by T3 (Fig. 2). The concentration of T3 that exhibited the maximum suppression of COL10A1 and Runx2, as well as the stimulation of COL2A1, was 100 nM. To further investigate the intracellular signaling involved, activation of Smads, p38 MAPK, and phosphatidylinositol-3 kinase/Akt, which are known to lie downstream of BMP-2 or insulin (34, 35) and also upstream of Runx2 (36, 37), was examined by Western blot analyses (Fig. 3*A*). The BMP receptor-specific Smad1/5/8, p38 MAPK, and Akt were phosphorylated 10, 10, and 5 min, respectively, after the treatment of BI. Although T3 (100 nM) hardly or faintly affected Smad or p38 MAPK activation by BI, it suppressed the Akt activation just like an Akt inhibitor. When we examined COL10A1 and Runx2 mRNA levels in the three-dimensional atelocollagen culture, both levels stimulated by BI were dose-dependently suppressed by the Akt inhibitor, similarly to those by T3 (Fig. 3*D*), suggesting that T3 prevented the BI-induced hypertrophic differentiation of redifferentiated chondrocytes at least partially via the suppression of the Akt signaling. The inhibitory effects of T3 or the Akt inhibitor on Akt activation by

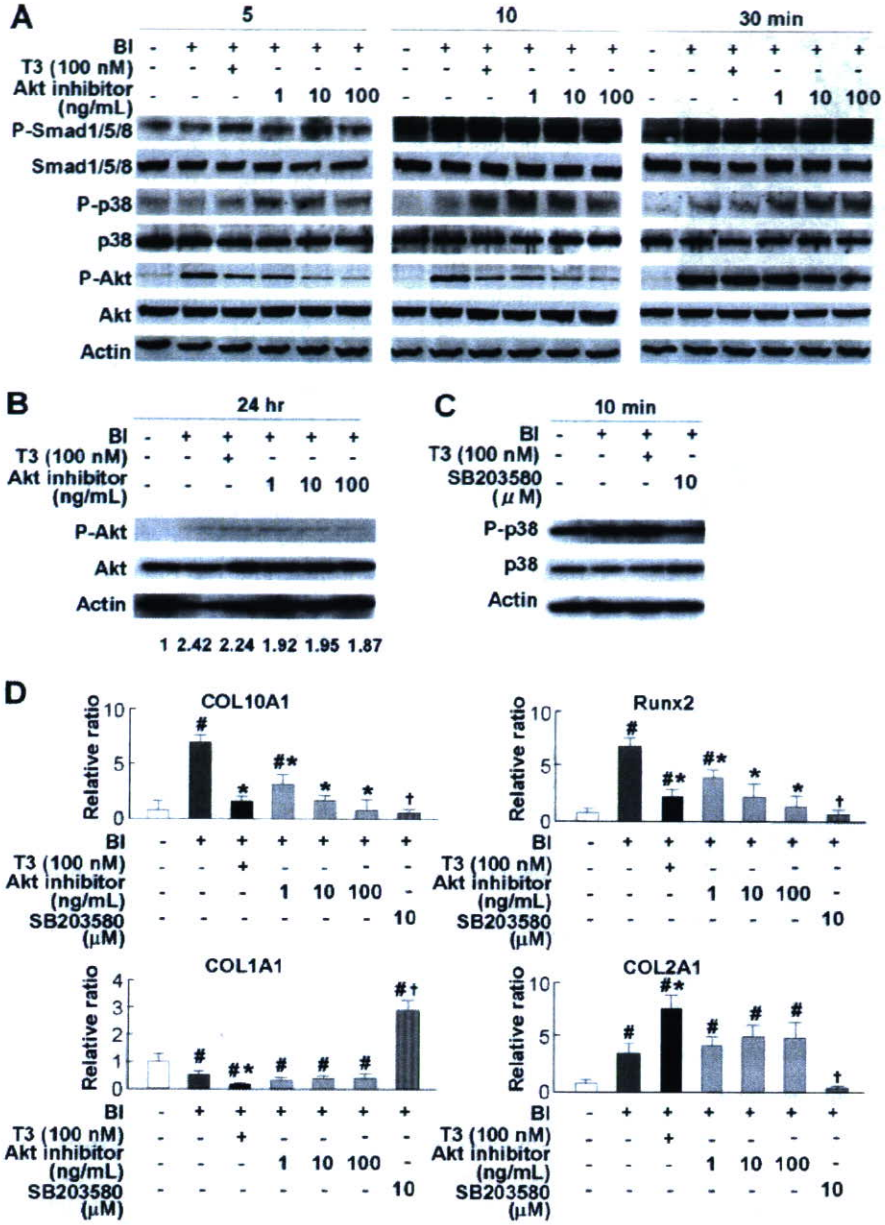

FIGURE 3. **Mechanism underlying the inhibitory effect of T3 on BI-induced hypertrophic differentiation of redifferentiated chondrocytes.** The dedifferentiated chondrocytes after multiplication in the monolayer culture underwent the three-dimensional culture under the stimulation. *A*, the effects of T3 (100 nM) or an Akt inhibitor (1–100 ng/ml) on phosphorylation of Smad 1/5/8 (*P-Smad 1/5/8*), p38 MAPK (*P-p38*), and Akt (*P-Akt*) in the three-dimensional atelocollagen culture for 5, 10, and 30 min. Western blottings were performed as described under "Experimental Procedures." *B*, the effects of T3 (100 nM) and the Akt inhibitor (1–100 ng/ml) on phosphorylation of Akt in the three-dimensional atelocollagen culture for 24 h. The *number* under each band is the p-Akt/Actin ratio of the intensity of each band measured by densitometry, which is scaled with control at 1. *C*, the effects of p38 MAPK inhibitor SB203580 (10 μM) on phosphorylation of p38 MAPK in the three-dimensional atelocollagen culture for 10 min. *D*, the effects of the Akt inhibitor (1–100 ng/ml) and the p38 MAPK inhibitor SB203580 (10 μM) on COL1A1, COL2A1, COL10A1, and Runx2 mRNA levels by real-time RT-PCR in the three-dimensional culture for 1 week. For *D*, data are expressed as mean (*bars*) ± S.E. (*error bars*) of relative ratios of the control culture for six cultures/group. #, $p < 0.01$, significant effects *versus* control; *, $p < 0.01$, significant effects by T3 or the Akt inhibitor *versus* BI; †, $p < 0.01$, significant effects by SB203508 *versus* BI.

BI continued for 24 h and then disappeared (Fig. 3*B*). Because the medium was changed twice/week throughout the experiment (1 week), T3 or the Akt inhibitor seemed to exert an inhibitory effect on the Akt activation in approximately one-third of the entire culture period and finally demonstrated the suppression of the Runx2 and Col10A1 expressions at the end of the culture (Fig. 3*D*). The phosphorylation of p38 MAPK seemed to be slightly increased by T3 (Fig. 3*A*), but the use of p38 MAPK inhibitor SB203580 instead of T3 rather down-regulated the expression of COL10A1 and RUNX2 (Fig. 3, *C* and *D*). The p38 inhibitor also suppressed that of COL2A1, but enhanced that of COL1A1, unlike T3 or the Akt inhibitor (Fig. 3*C*), suggesting that the slight up-regulation of the p38 MAPK activation by T3 may be associated not with chondrocyte hypertrophy but with enhancement of the early chondrocyte differentiation markers such as the collage type II or proteoglycan.

Properties of the Tissue-engineered Cartilage from Human Chondrocytes by BIT—We next examined the properties of the tissue-engineered cartilage pellet generated by the three-dimensional atelocollagen culture (2×10^5 cells/20 μl) with and without stimulation by BI or BIT from human auricular chondrocytes that were dedifferentiated after long term monolayer culture, as described above. The size of pellets with BI or BIT stimulation was much larger than that without stimulation (Fig. 4*A*, *top*). In addition, histological analyses of toluidine blue staining revealed more proteoglycan production shown by metachromasia with cartilage lacunae under the BI stimulation as compared with the control, which was further enhanced by BIT (Fig. 4*A*, *bottom*). Measurement of cartilaginous matrix protein levels also revealed that the redifferentiation markers GAG and COL2, but not the dedifferentiation marker COL1, were stimulated moderately by BI and strongly by BIT (Fig. 4*B*). However, the GAG level tended to be lower in all these groups as compared with that in native cartilage (Fig. 4*B*). The ratio of GAG/COL1 and that of COL2/COL1 were 0.77 ± 0.25 and 0.49 ± 0.64, respectively, for the control, 4.12 ± 0.94/1.47 ± 0.96 for BI and 5.16 ± 1.57/4.44 ± 1.66 for BIT, which successively approached the value of the native cartilage (9.37 ± 3.26/6.06 ± 3.15). The cell proliferation determined by proliferating cell nuclear antigen and cyclin D1 mRNA levels was significantly decreased by BI and

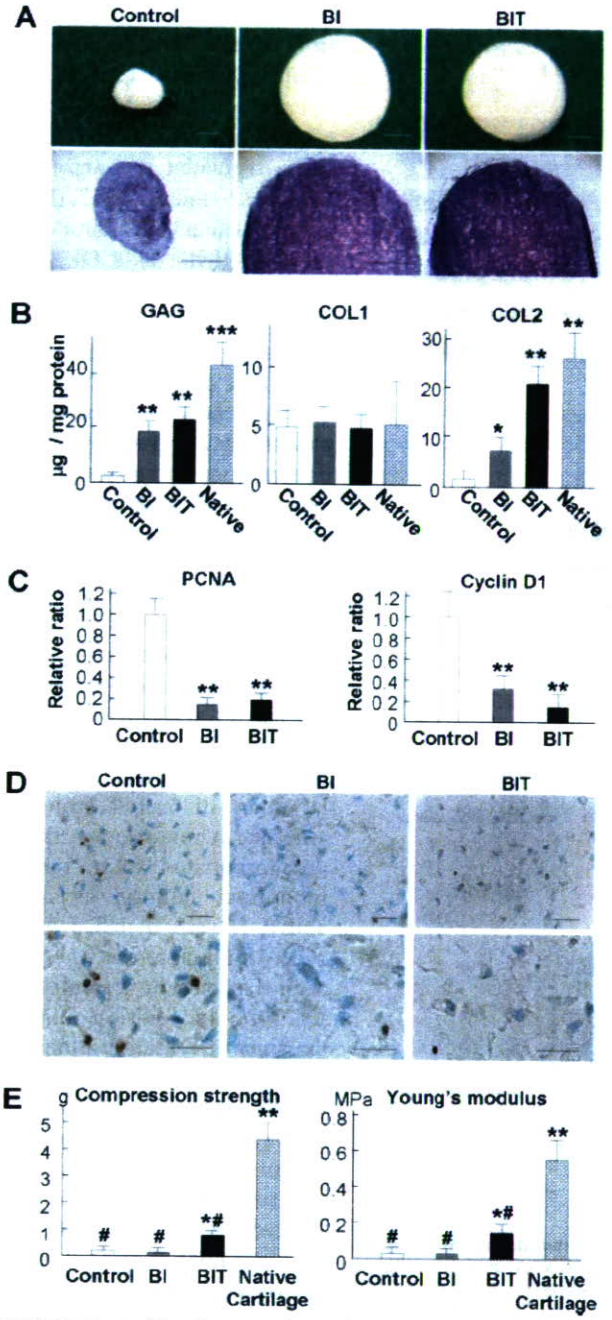

FIGURE 4. **Analyses of the tissue-engineered cartilage pellet by three-dimensional atelocollagen culture with and without stimulation by BI or BIT.** *A*, macroscopic (*top*) and histological findings stained with toluidine blue-O (*bottom*) after 3 weeks of the three-dimensional atelocollagen culture. *Scale bars*, 1 mm (*top*) and 100 μm (*bottom*). *B*, GAG, COL1, and COL2 protein levels after 3 weeks of the three-dimensional culture. Data are expressed as mean (*bars*) ± S.E. (*error bars*) for six samples/group. *Native*, native human auricular cartilage. *, $p < 0.05$, **, $p < 0.01$, ***, $p < 0.001$, significant effects *versus* control. *C*, proliferating cell nuclear antigen (*PCNA*) and cyclin D1 mRNA levels in the pellet after 1 week of the three-dimensional culture. Data are expressed as mean (*bars*) ± S.E. (*error bars*) of relative ratios of the control culture for six cultures/group. **, $p < 0.01$, significant effects *versus* control. *D*, TUNEL staining in the middle area of the pellet after 1 week of the three-dimensional culture. The *bottom* is under a higher magnification than the *top*. The nuclei were densely stained in the apoptotic cells. *Scale bar*, 20 μm. *E*, mechanical properties of the pellet after 3 weeks of the three-dimensional culture determined by compression strength and Young's modulus as compared with the native human auricular cartilage. Data are expressed as mean (*bars*) ± S.E. (*error bars*) for six samples/group. *, $p < 0.05$, **, $p < 0.01$, significant effects *versus* control. #, $p < 0.01$, significant difference from the native cartilage.

BIT, suggesting that these stimulations did not cause cell cycle acceleration or carcinogenesis (38) (Fig. 4*C*). Contrarily, the cell apoptosis shown by TUNEL staining was decreased by BI and BIT (Fig. 4*D*). We further examined the mechanical properties of the pellets using a tactile sensor and compared them with those of the native auricular cartilage of microtia patients taken as surgical specimens (Fig. 4*E*). Although the mechanical properties of the BIT-treated cartilage were significantly greater than those of the control and BI-treated ones, they were much less than those of the native human auricular cartilage.

Aiming at regenerating permanent cartilage that is applicable for clinical use, we created implants by adding the human auricular chondrocytes cultured in the three-dimensional atelocollagen gel to the PLLA mesh scaffold (10^6 cells/columnar implant 10 mm in diameter and 1 mm in thickness). The implants were cultured for 3 weeks with and without stimulation by BI or BIT (Fig. 5*B*, *top*) and thereafter transplanted subcutaneously into nude mice for 2 months (Fig. 5*A*). Although the size of the excised implants of the three groups seemed similar (Fig. 5*B*, *bottom*), depending on the original PLLA scaffold size, the metachromatic proteoglycan production was much more enhanced in the BIT-treated implant than in the other two groups (Fig. 5*C*). The implants of the control (Fig. 5*D*, *Control*) and BI (data not shown) groups contained not only hyaline cartilage with COL2-like fibrils but also fibrous cartilage with COL1-like fibrils even in the center of the implants, showing the mingling with the hyaline cartilage and fibrous one. However, the BIT-treated implants were filled with hyaline cartilage (Fig. 5*D*, *BIT*). Biochemical analyses confirmed the advantages of BIT: that GAG and COL2, but not COL1, were significantly stimulated by the treatment (Fig. 5*E*). The GAG level in the BIT reached that of the native cartilage, whereas COL2 in BIT tended to be higher than in the native one (Fig. 5*E*). The ratio of GAG/COL1 and that of COL2/COL1 were 0.44 ± 0.18 and 0.25 ± 0.18, respectively, for the control, 0.78 ± 0.43/0.71 ± 0.23 for BI, and 1.61 ± 0.61/1.68 ± 0.61 for BIT. The decrease in these ratios as compared with those of the tissue-engineered cartilage pellets cultured *in vitro* or the native cartilage may be due to the difficulty in the removal of the COL1-based fibrous tissues around the *in vivo* regenerated cartilage. Here again, COL10-positive matrices were visible only in the BI-treated implant but not in the control or BIT-treated one (Fig. 5*F*). Furthermore, mechanical parameters of the control, BI-, and BIT-treated implants were higher than those of the PLLA scaffold without cultured cells (Fig. 5*G*). Among them, both parameters of the BIT-treated cartilage were not only greater than the control and BI-treated cartilage but also comparable with that of the native cartilage.

DISCUSSION

The present study succeeded in overcoming the two major limitations of tissue engineering of permanent cartilage from autologous human chondrocytes: dedifferentiation during the long term culture for multiplication and hypertrophic differentiation by stimulation for redifferentiation. For the efficient and exhaustive search for the optimal combination, we utilized the analysis of variance by the fractional factorial design (9). This method was originally developed in the agricultural science

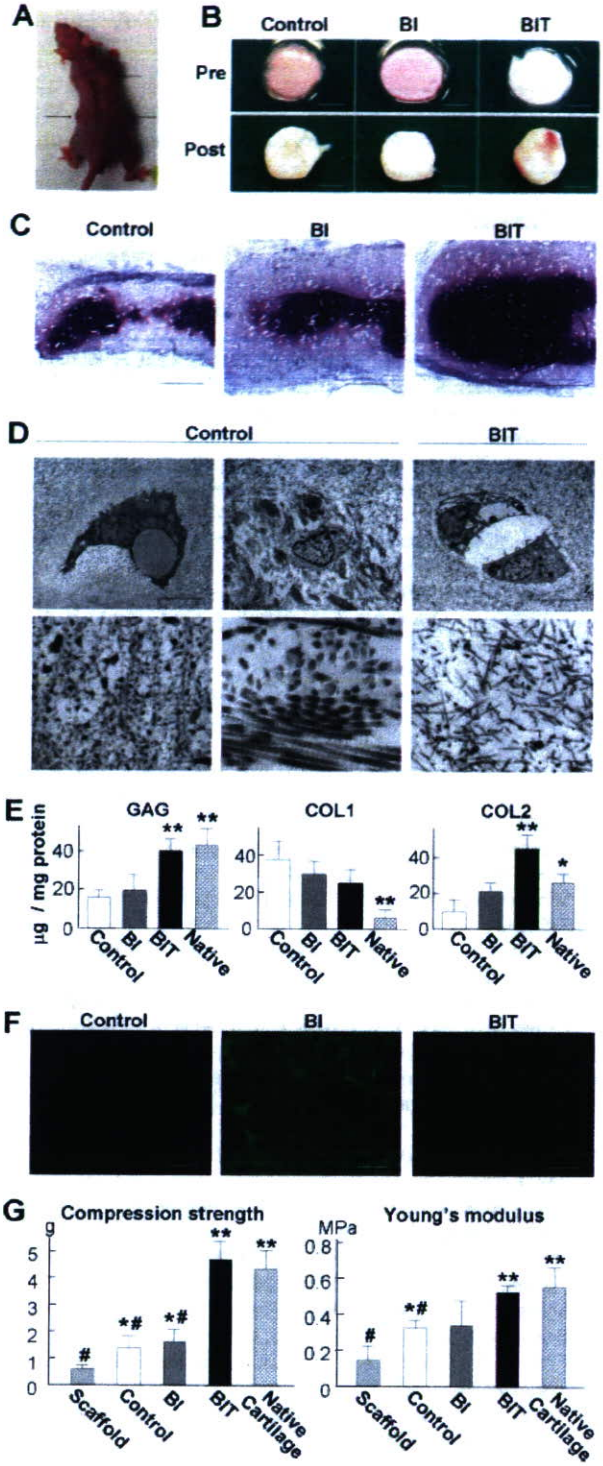

FIGURE 5. **Analyses of the tissue-engineered cartilage implants.** *A*, the implants were generated by human auricular chondrocytes that underwent the long term monolayer culture followed by 3-week three-dimensional culture in the atelocollagen gel and the PLLA mesh scaffold with and without stimulations by BI or BIT, and further, by 2-month subcutaneous implantation in nude mice. *B*, macroscopic findings of the implants before (*Pre*) and after (*Post*) the *in vivo* transplantation. *Scale bars*, 5 mm. *C*, histological findings of the coronal section of the implants after the *in vivo* transplantation (toluidine blue-O staining). *Scale bars*, 0.5 mm. *D*, electron microscopic findings in the middle area of the implants after the *in vivo* transplantation. *Scale bars*, 10 μm and 100 nm for lower (*top*) and higher (*bottom*) magnifications, respectively. *E*, GAG, COL1, and COL2 protein levels in the implants after the *in vivo* transplantation. Data are expressed as mean (*bars*) ± S.E. (*error bars*) for six implants/group. *Native*, native human auricular cartilage. *, $p < 0.05$, **, $p < 0.01$, significant effects *versus* control. *F*, immunostainings with an anti-COL10 antibody in the middle area of the implants. *Scale bar*, 50 μm. *G*, mechanical properties of the implants after the *in vivo* transplantation, determined by compression strength and Young's modulus, as compared with the PLLA scaffold alone and the native human auricular cartilage. Data are expressed as mean (*bars*) ± S.E. (*error bars*) for six implants/group. *, $p < 0.05$, **, $p < 0.01$, significant difference from the scaffold alone. #, $p < 0.01$, significant difference from the native cartilage.

field; one could decide the optimal conditions to yield good crops out of many naturally fluctuating conditions including temperature, soil condition, rainfall, etc (39). Thereafter, this method was successfully adapted to industrial applications; *e.g.* it drastically reduced production errors of aircraft engine manufacturing to one-fifth through the grading of numerous parameters including cutting oil, cutting speed, groove ratio, tip-end angle, etc (40). Since this method is now widely approved as being useful for the maintenance of goods and services of high quality, the Food and Drug Administration Good Manufacturing Practices regulation and the International Organization for Standardization 9000 series now require its confirmation for process validation (9). This method, however, has not been applied for quality control in medical fields that contain tremendous parameter variations. The present study for the first time adopted the method to determine the optimal combination of putative factors for a regenerative medicine and demonstrated its usefulness.

BMP-2 was shown to have the strongest potency to produce GAG as a single factor, according to the result of analysis of variance by the fractional factorial design (Fig. 1*A*). BMP-2 is known to enhance not only chondrogenic differentiation but also further hypertrophic differentiation of chondrocytes in several cell cultures (7, 20), which is a critical weakness for the regeneration of permanent cartilage. Insulin is also reported to induce both chondrogenic and hypertrophic differentiation in cultures (11). The third factor, T3, as well as its prohormone L-thyroxin (T4), are also known to play important roles in physiological skeletal growth by regulating terminal differentiation of chondrocytes. A childhood hypothyroidism, congenital hypothyroidism, is characterized by growth arrest and short stature, whereas childhood thyrotoxicosis causes accelerated growth and premature closure of the growth plate (41). Mice devoid of all isoforms produced from thyroid hormone receptor-α ($TR\alpha^{0/0}$) exhibited dwarfism due to impaired hypertrophic differentiation of chondrocytes in the growth plate (42). In addition, several *in vitro* studies have shown that T3 around physiological concentrations (0.1–1 nM) stimulates the terminal differentiation markers COL10, alkaline phosphatase, and osteopontin in several chondrocyte culture systems (43, 44). These seem to be inconsistent with the present finding that T3 prevented BI from inducing hypertrophic differentiation through suppression of the phosphatidylinositol-3 kinase/Akt signaling, a major pathway for chondrocyte differentiation (34). The thyroid hormones are generally believed to exert their functions through the genomic action by activating the nuclear receptors (TRα1 and -2 and TRαβ1, -2, and -3), causing a conformational change that leads to dissociation from a repressor complex and interaction with an activation complex containing

histone acetylase (41). In contrast, T3 at higher concentrations has been suggested to exert a nongenomic action; *e.g.* T3 (0.1–100 μM) caused a rapid activation of the Na^+/H^+ exchanger activity in isolated rat alveolar type II cells or rat AT II cell line RLE-6TN (45). The present study showed that T3 at more than 100 nM caused inhibition of COL10 and Runx2 expressions with a rapid suppression of Akt phosphorylation induced by BI within 5 min. We speculate that the T3 action might be a nongenomic one that is somehow associated with the BI and Runx2 signalings. In Fig. 2, Sox9 that is a potent inhibitor of the chondrocyte hypertrophy (32) was down-regulated in BI, implying the induction of chondrocyte hypertrophy in BI. However, the addition of T3 to BI did not up-regulate the Sox9 expression, which may not follow the effect of BIT on the inhibition of the chondrocyte hypertrophy. It was reported that the thyroid hormone around the physiological concentration (T4, 30 ng/ml) inhibited the Sox9 expression and promoted chondrocyte hypertrophy in the rat chondrocyte pellet culture (46). These functions of the thyroid hormone around the physiological concentration seemed to work through a genomic action (44). The decrease in the Sox9 expression by the addition of 10^{-7} M T3 in the present experiment may suggest that T3 down-regulated the expression of Sox9 through the genomic action, even at the pharmacological concentration. However, we think that T3 at the pharmacological concentration prevents hypertrophic differentiation mainly through a nongenomic machinery. The nongenomic effect may dominate the genomic action in the pharmacological condition, leading to the inhibition of chondrocyte hypertrophy.

Considering that some tens to 100 ml of regenerated cartilage is necessary for its clinical application to major skeletal disorders with severe cartilage defects, we should initially obtain a sufficient number of cells from a limited amount of specimen that is no more than 0.1 ml (10^6 cells), meaning that a 1,000-fold increase in cell number is needed. For efficient cell proliferation, many researchers have performed cell cultures with mitogenic growth factors in the presence of fetal bovine serum that is unfavorable for clinical use due to the risk of pathogen transmission and immune reaction (47). Previous trials of cultures using autologous human serum, however, could provide no more than 10^7 cells, which corresponds to at most 1 ml of regenerative cartilage (2, 3). To overcome this problem, our preparatory study established a fetal bovine serum-free culture system of primary human chondrocytes that realize a 1,000-fold increase in cell number within 4 weeks under the stimulation of FGF-2 with insulin or IGF-I (8), although the cell dedifferentiation was inevitable during the repeated passaging. Based on the previous study, the present study further established a serum-free culture system that causes redifferentiation of the dedifferentiated cells and maintains the properties of permanent cartilage. Since we succeeded in regenerating a high quality cartilage column 10 mm in diameter and 1 mm in thickness that is ~80 μl in volume, starting from 10^3 primary chondrocytes in a surgical specimen, it is estimated that 80 ml of cartilage can be regenerated from 0.1 ml of a specimen containing 10^6 cells by using our original two systems. We conclude that the BIT stimulation realized the tissue engineering of permanent cartilage whose quantity and quality satisfy the revolutionary treatment of major skeletal disorders. A clinical trial is now underway.

Acknowledgments—We thank Dr. Yoshiro Takano, Satoru Nishizawa, and Takashi Nakamoto for technical support and useful discussion.

REFERENCES

1. Brittberg, M., Lindahl, A., Nilsson, A., Ohlsson, C., Isaksson, O., and Peterson, L. (1994) *N. Engl. J. Med.* **331,** 889–895
2. Ochi, M., Uchio, Y., Kawasaki, K., Wakitani, S., and Iwasa, J. (2002) *J. Bone Jt. Surg. Br.* **84,** 571–578
3. Peterson, L., Minas, T., Brittberg, M., and Lindahl, A. (2003) *J. Bone Jt. Surg. Am.* **85,** S17–24
4. von der Mark, K., Gauss, V., von der Mark, H., and Muller, P. (1977) *Nature* **267,** 531–532
5. Grunder, T., Gaissmaier, C., Fritz, J., Stoop, R., Hortschansky, P., Mollenhauer, J., and Aicher, W. K. (2004) *Osteoarthritis Cartilage* **12,** 559–567
6. Tallheden, T., Karlsson, C., Brunner, A., Van Der Lee, J., Hagg, R., Tommasini, R., and Lindahl, A. (2004) *Osteoarthritis Cartilage* **12,** 525–535
7. Valcourt, U., Gouttenoire, J., Moustakas, A., Herbage, D., and Mallein-Gerin, F. (2002) *J. Biol. Chem.* **277,** 33545–33558
8. Takahashi, T., Ogasawara, T., Kishimoto, J., Liu, G., Asato, H., Nakatsuka, T., Nakamura, K., Kawaguchi, H., Chung, U. I., Takato, T., and Hoshi, K. (2005) *Cell Transplant.* **14,** 683–693
9. Berling, T., and Runeson, P. (2003) *IEEE Trans. Software Eng.* **29,** 769–781
10. Ushida, T., Furukawa, K., Toita, K., and Tateishi, T. (2002) *Cell Transplant.* **11,** 489–494
11. Kato, Y., and Gospodarowicz, D. (1984) *J. Cell Physiol.* **120,** 354–363
12. Grigoriadis, A. E., Aubin, J. E., and Heersche, J. N. (1989) *Endocrinology* **125,** 2103–2110
13. Monsonego, E., Halevy, O., Gertler, A., Hurwitz, S., and Pines, M. (1995) *Mol. Cell. Endocrinol.* **114,** 35–42
14. Wroblewski, J., and Edwall-Arvidsson, C. (1995) *J. Bone Miner. Res.* **10,** 735–742
15. Malinin, T. I., and Hornicek, F. J. (1997) *Transplant. Proc.* **29,** 2037–2039
16. Maor, G., Segev, Y., and Phillip, M. (1999) *Endocrinology* **140,** 1901–1910
17. Zerega, B., Cermelli, S., Bianco, P., Cancedda, R., and Cancedda, F. D. (1999) *J. Bone Miner. Res.* **14,** 1281–1289
18. Yasuda, T., and Poole, A. R. (2002) *Arthritis Rheum.* **46,** 138–148
19. Rodd, C., Jourdain, N., and Alini, M. (2004) *Calcif. Tissue Int.* **75,** 214–224
20. Shukunami, C., Ohta, Y., Sakuda, M., and Hiraki, Y. (1998) *Exp. Cell Res.* **241,** 1–11
21. Li, J., Kim, K. S., Park, J. S., Elmer, W. A., Hutton, W. C., and Yoon, S. T. (2003) *J. Orthop. Sci.* **8,** 829–835
22. Stevens, R. L., Nissley, S. P., Kimura, J. H., Rechler, M. M., Caplan, A. I., and Hascall, V. C. (1981) *J. Biol. Chem.* **256,** 2045–2052
23. Bohme, K., Conscience-Egli, M., Tschan, T., Winterhalter, K. H., and Bruckner, P. (1992) *J. Cell Biol.* **116,** 1035–1042
24. Crabb, I. D., O'Keefe, R. J., Puzas, J. E., and Rosier, R. N. (1992) *Calcif. Tissue Int.* **50,** 61–66
25. Arend, W. P., Welgus, H. G., Thompson, R. C., and Eisenberg, S. P. (1990) *J. Clin. Investig.* **85,** 1694–1697
26. Ohlsson, C., Nilsson, A., Swolin, D., Isaksson, O. G., and Lindahl, A. (1993) *Mol. Cell. Endocrinol.* **91,** 167–175
27. Mackintosh, D., and Mason, R. M. (1988) *Biochim. Biophys. Acta* **964,** 295–302
28. Schwartz, Z., Knight, G., Swain, L. D., and Boyan, B. D. (1988) *J. Biol. Chem.* **263,** 6023–6026
29. Aoyagi, R., and Yoshida, T. (2004) *Jpn. J. Appl. Phys.* **43,** 3204–3209
30. Inada, M., Yasui, T., Nomura, S., Miyake, S., Deguchi, K., Himeno, M., Sato, M., Yamagiwa, H., Kimura, T., Yasui, N., Ochi, T., Endo, N, Kitamura, Y., Kishimoto, T., and Komori, T. (1999) *Dev. Dyn.* **214,** 279–290
31. de Crombrugghe, B., Lefebvre, V., and Nakashima, K. (2001) *Curr. Opin. Cell Biol.* **13,** 721–727

32. Akiyama, H., Chaboissier, M. C., Martin, J. F., Schedl, A., and de Crombrugghe, B. (2002) *Genes Dev.* **16,** 2813–2828
33. Chung, U., and Kronenberg, H. (2000) in *Skeletal Growth Factors* (Canalis, E., ed) pp. 355–364, Lippincott Williams and Wilkins, Philadelphia, PA
34. Hidaka, K., Kanematsu, T., Takeuchi, H., Nakata, M., Kikkawa, U., and Hirata, M. (2001) *Int. J. Biochem. Cell Biol.* **33,** 1094–1103
35. Nohe, A., Keating, E., Knaus, P., and Petersen, N. O. (2004) *Cell. Signal.* **16,** 291–299
36. Leboy, P., Grasso-Knight, G., D'Angelo, M., Volk, S. W., Lian, J. V., Drissi, H., Stein, G. S., and Adams, S. L. (2001) *J. Bone Jt. Surg. Am.* **83,** S15–22
37. Fujita, T., Azuma, Y., Fukuyama, R., Hattori, Y., Yoshida, C., Koida, M., Ogita, K., and Komori, T. (2004) *J. Cell Biol.* **166,** 85–95
38. Shamma, A., Doki, Y., Shiozaki, H., Tsujinaka, T., Yamamoto, M., Inoue, M., Yano, M., and Monden, M. (2000) *Int. J. Oncol.* **16,** 261–266
39. Kim, J., and Kalb, J. (1996) *Med. Device Diagn. Ind.* **18,** 78–90
40. Fujimoto, R. (2003) *IHI Engineering Review* **36,** 168–172
41. Bassett, J. H., and Williams, G. R. (2003) *Trends Endocrinol. Metab.* **14,** 356–364
42. Gauthier, K., Plateroti, M., Harvey, C. B., Williams, G. R., Weiss, R. E., Refetoff, S., Willott, J. F., Sundin, V., Roux, J. P., Malaval, L., Hara, M., Samarut, J., and Chassande, O. (2001) *Mol. Cell. Biol.* **21,** 4748–4760
43. Ballock, R. T., and Reddi, A. H. (1994) *J. Cell Biol.* **126,** 1311–1318
44. Miura, M., Tanaka, K., Komatsu, Y., Suda, M., Yasoda, A., Sakuma, Y., Ozasa, A., and Nakao, K. (2002) *J. Bone Miner. Res.* **17,** 443–454
45. Lei, J., Nowbar, S., Mariash, C. N., and Ingbar, D. H. (2003) *Am. J. Physiol.* **285,** L762–L772
46. Okubo, Y., and Reddi, A. H. (2003) *Biochem. Biophys. Res. Commun.* **306,** 186–190
47. Johnson, L. F., deSerres, S., Herzog, S. R., Peterson, H. D., and Meyer, A. A. (1991) *J. Burn Care Rehabil.* **12,** 306–312

Enhanced Wear Resistance of Orthopaedic Bearing Due to the Cross-Linking of Poly(MPC) Graft Chains Induced by Gamma-Ray Irradiation

Masayuki Kyomoto,[1,2] Toru Moro,[3] Fumiaki Miyaji,[1] Tomohiro Konno,[2] Masami Hashimoto,[4] Hiroshi Kawaguchi,[3] Yoshio Takatori,[3] Kozo Nakamura,[3] Kazuhiko Ishihara[2]

[1] Research Division, Japan Medical Materials Corporation, Osaka, Japan

[2] Department of Materials Engineering, School of Engineering and Center for NanoBio Integration, The University of Tokyo, Tokyo, Japan

[3] Department of Orthopaedic Surgery, School of Medicine, The University of Tokyo, Tokyo, Japan

[4] Materials Research and Development Laboratory, Japan Fine Ceramics Center, Nagoya, Japan

Received 17 January 2007; revised 31 March 2007; accepted 30 April 2007
Published online 22 June 2007 in Wiley InterScience (www.interscience.wiley.com). DOI: 10.1002/jbm.b.30874

Abstract: We assumed that the extra energy supplied by gamma-ray irradiation produced cross-links in 2-methacryloyloxyethyl phosphorylcholine (MPC) polymer grafted cross-linked polyethylene (CLPE-*g*-MPC) and investigated its effects on the tribological properties of CLPE-*g*-MPC. In this study, we found that the gamma-ray irradiation produced cross-links in three kinds of regions of CLPE-*g*-MPC: poly(MPC) layer, CLPE-MPC interface, and CLPE substrate. The dynamic coefficient of friction of CLPE-*g*-MPC slightly increased with increasing irradiation doses. After the simulator test, both the nonsterilized and gamma-ray sterilized CLPE-*g*-MPC cups exhibited lower wear than the untreated CLPE ones. In particular, the gamma-ray sterilized CLPE-*g*-MPC cups showed extremely low and stable wear. As for the nonsterilized CLPE-*g*-MPC cups, the weight change varied with each cup. When the CLPE surface is modified by poly(MPC) grafting, the MPC graft polymer leads to a significant reduction in the sliding friction between the surfaces that are grafted because water thin films formed can behave as extremely efficient lubricants. Such a cross-link of poly(MPC) slightly increases the friction of CLPE by gamma-ray irradiation but provides a stable wear resistant layer on the friction surface. The cross-links formed by gamma-ray irradiation would give further longevity to the CLPE-*g*-MPC cups. © 2007 Wiley Periodicals, Inc. J Biomed Mater Res Part B: Appl Biomater 84B: 320–327, 2008

Keywords: joint replacements; polyethylene; phosphorylcholine; sterilization

INTRODUCTION

The number of primary and revised artificial hip and knee joints used are substantially increasing in the world every year.[1] This means that the quality of artificial joints has been becoming increasingly important. Most of the patients who receive an artificial joint experience a dramatic pain relief and enjoy a rapid improvement in the quality of life. The most popular artificial joint system is a bearing couple composed of an ultra-high molecular weight polyethylene (UHMWPE) and Co-Cr-Mo alloy. However, osteolysis caused by wear particles of UHMWPE has emerged as a serious issue.[2–4] The reduction in the number of UHMWPE wear particles is a method to prevent osteolysis. From this viewpoint, different combinations of bearing surfaces and improvement in the bearing materials have been focused upon.

We have recently developed a novel artificial joint system with 2-methacryloyloxyethyl phosphorylcholine (MPC) polymer grafted onto the surface of cross-linked polyethylene (CLPE-*g*-MPC),[5–7] aiming to reduce wear and avoid bone resorption. MPC is a methacrylate monomer that has a phospholipid polar group in a side chain and is used to make novel biomaterials as designed by Ishihara et al., who were inspired by the natural phospholipids of biomembranes.[8] MPC can be a good polymer biomaterial owing to

Correspondence to: M. Kyomoto (e-mail: kyomotom@jmmc.jp)
Contract grant sponsor: Japanese Ministry of Education, Culture, Sports, Science, and Technology; Contract grant number: 15390449
Contract grant sponsor: Japanese Ministry of Health, Labour, and Welfare

the reduction of protein adsorption and cell adhesion.[9–18] On the basis of the biocompatibility and hydrophilicity of MPC polymers, we have been developing new artificial joints with highly lubricated bearing surfaces that are produced by photo-induced radical graft polymerization.[19] This technique grafts MPC directly onto CLPE, forming C—C covalent bonds between the CLPE substrate and the MPC polymer.

Medical devices, including artificial joints, are normally sterilized by using several methods, for example, gamma-ray sterilization, ethylene oxide gas sterilization, and gas plasma sterilization. In particular, gamma-ray irradiation is the sterilization method typically used for the UHMWPE components of artificial joints. However, gamma-ray sterilization probably influences the properties of medical devices. Generally, when a high energy beam generated by gamma-ray sterilization is irradiated on to a polymer, free radicals are formed by the scission of the molecular chains. This is followed by the retermination and cross-linking of the molecules. The irradiation of high-dose gamma-rays onto UHMWPE severs the C—C or C—H bonds, and it then produces cross-linking and subsequent chemical bonding involving C=O and C—C.[20] It has been reported that gamma-ray sterilized UHMWPE sometimes exhibits improved wear resistance due to the formation of many cross-links. Several investigators have reported that wear resistance is better in gamma-ray sterilized UHMWPE than that in ethylene oxide sterilized UHMWPE.[21–24]

The purpose of this study is to investigate the dependence of gamma-ray irradiation on the tribological (friction and *in vitro* wear) properties of CLPE-*g*-MPC and to examine the possibility of controlling the longevity of artificial joints by using this material. This is based on the hypothesis that the extra energy supplied by gamma-ray irradiation could produce cross-links in CLPE-*g*-MPC.

MATERIALS AND METHODS

Chemicals and MPC Graft Polymerization

Benzophenone and acetone were purchased from Wako Pure Chemical Industries (Osaka, Japan). MPC was industrially synthesized using the method reported by Ishihara et al.[8] and was supplied by Ai Bio-Chips (Tokyo, Japan).

A compression-molded UHMWPE (GUR1020 resin, Poly Hi-Solidur, IN) bar stock was treated with a dose of 50 kGy gamma irradiation in N_2 gas and annealed at 120°C for 7.5 h in N_2 gas in order to attain cross-linking. The CLPE specimens were machined from this bar stock after cooling. They were immersed in an acetone solution containing 10 mg/mL benzophenone for 30 s and then dried in the dark at room temperature to remove acetone. The amount of benzophenone adsorbed on the surface was 3.5×10^{-11} mol/cm^2.[25] The MPC monomer was dissolved in pure degassed water up to a concentration of 0.5 mol/L. The CLPE specimens coated with benzophenone were immersed in the aqueous MPC solution. The photo-induced graft polymerization on the CLPE surface was carried out with an ultraviolet irradiation (UVL-400HA ultra-high pressure mercury lamp, Riko-Kagaku Sangyo, Funabashi, Japan) of 5 mW/cm^2 at 60°C for 90 min using a filter (Model D-35; Toshiba, Tokyo, Japan) to pass only ultraviolet light with a wavelength of 350 ± 50 nm. After the polymerization, the CLPE-*g*-MPC specimens were removed, washed with pure water and ethanol, and dried at room temperature. The CLPE and CLPE-*g*-MPC specimens were sterilized by gamma-ray irradiation of 25 or 50 kGy in N_2 gas.

Surface Analysis by Fourier-Transform Infrared and X-ray Photoelectron Spectroscopies and Water-Contact Angle Measurement

The functional group vibrations of both the nonsterilized and gamma-ray sterilized CLPE and CLPE-*g*-MPC surfaces were examined by Fourier-transform infrared (FTIR) spectroscopy using attenuated total reflection (ATR) equipment. The FTIR/ATR spectra were obtained in 32 scans over a range of 800–2000 cm^{-1} using an FTIR analyzer (FT/IR-615; JASCO International, Tokyo, Japan) at a resolution of 4.0 cm^{-1}.

The surface elemental conditions of CLPE before and after MPC grafting were analyzed by X-ray photoelectron spectroscopy (XPS). The XPS spectra were obtained using an XPS spectrophotometer (AXIS Hsi 165; Kratos Analytical, UK) equipped with an Mg-Kα radiation source at 15 kV at the anode. The take-off angle of the photoelectrons was kept at 90°. Each sample was scanned five times.

The static water-contact angles of CLPE-*g*-MPC with various photo-polymerization periods were measured by a sessile drop method using an optical bench-type contact angle goniometer (Model DM300; Kyowa Interface Science, Saitama, Japan). Drops of purified water (1 μL) were deposited onto the surface of CLPE-*g*-MPC, and the contact angles were directly measured by using a microscope after 60 s according to the ISO 15989 standard.[26] Fifteen replicate measurements were performed on each sample, and the average values were taken as contact angles.

Friction Test

The friction test was performed using a ball-on-plate machine (Tribostation 32; Shinto Scientific, Tokyo, Japan). Six sample pieces were prepared using each of the sterilization methods. The Co-Cr-Mo alloy ball was 9 mm in diameter and its surface roughness was Ra $\geq$ 0.01—as smooth as a femoral ball. The friction tests were carried out with a load of 0.98 N and a sliding distance of 25 mm with a frequency of 1 Hz at room temperature. The measurements were performed using pure water as lubricant. The friction tests were performed up to a maximum of 100 cycles. The mean static (μ_s) and dynamic (μ_d) coefficients of friction were determined by averaging five data points in 10 (8–12) and 100 (96–100) cycle measurements.

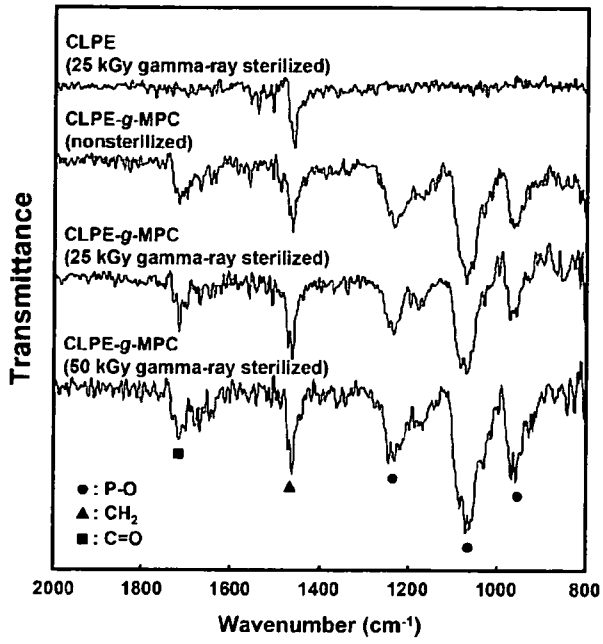

Figure 1. FTIR/ATR spectra for nonsterilized and gamma-ray sterilized CLPE and CLPE-*g*-MPC.

Statistical Analysis

For the water-contact angle measurement and friction test, the results derived from each measurement were expressed as mean values and the standard deviation. The statistical significance ($p < 0.05$) was judged by the Student's *t*-test.

Hip Joint Simulator Test

The inner and outer diameters of the CLPE and CLPE-*g*-MPC cups used in the hip joint simulator were 26 and 52 mm, respectively. Four pieces for each condition was prepared. The wear test was performed using a 12-station hip joint simulator (MTS Systems, MN). A Co-Cr-Mo alloy femoral ball component with a size of 26 mm (Japan Medical Materials, Osaka, Japan) was used as *a femoral* component. A mixture of 25 vol % bovine serum, 20 mM/L of ethylene diamine tetraacetic acid (EDTA), and 0.1 mass % sodium azide was used as lubricant, according to the ISO 14242-1 standard.[27] The lubricant was replaced every 0.5 $\times 10^6$ cycles. Loads simulating a physiologic loading curve with double peaks of 1793 and 2744 N loads were applied with a frequency of 1 Hz. The wear was determined by weighing the polyethylene cups. Load-soak controls ($n = 2$) were used to compensate the fluid absorption of specimens. The weights of the cups were measured every 0.5×10^6 cycles. Then, the testing was continued until a total of 5.0×10^6 cycles were completed.[28]

To evaluate the wear conditions, the surface features of the bearing surfaces of the cups were observed with a confocal laser scanning microscope (OLS1200; Olympus, Tokyo, Japan) after a simulator test with 5.0×10^6 cycles.

RESULTS

Figure 1 shows the FTIR/ATR spectra for the nonsterilized and gamma-ray sterilized CLPE and CLPE-*g*-MPC. An absorption peak was observed at 1460 cm^{-1} for both CLPE and CLPE-*g*-MPC. This peak is attributed mainly to the methylene chain in the CLPE substrate and MPC graft polymer. However, the transmission absorptions at 1240, 1080, and 970 cm^{-1} were observed only for the CLPE-*g*-MPC. These peaks are due to the phosphate group in the MPC unit. Similarly, an absorption peak at 1720 cm^{-1} observed for CLPE-*g*-MPC only corresponds to the carbonyl group in the MPC unit. The FTIR/ATR spectra did not differ significantly between the nonsterilized and gamma-ray sterilized CLPE-*g*-MPC.

Table I summarizes the elemental compositions of the untreated CLPE and the nonsterilized and gamma-ray sterilized CLPE-*g*-MPC surfaces. Both the elemental composition of nitrogen and phosphorous in the nonsterilized and gamma-ray sterilized CLPE-*g*-MPC surface were approximately 5.2. It should be noted that the contents of nitrogen and phosphorous in the CLPE-*g*-MPC surface remained unchanged after gamma-ray sterilization. The elemental composition of the CLPE-*g*-MPC surface was almost equivalent to the theoretical elemental composition (N = 5.3, P = 5.3) of poly(MPC). On the other hand, the carbon content in the gamma-ray sterilized CLPE-*g*-MPC slightly increased as compared with that of the nonsterilized one.

Figure 2 shows the static water-contact angle of the untreated CLPE and the nonsterilized and gamma-ray sterilized CLPE-*g*-MPC surfaces. The static water-contact angle

TABLE I. Surface Elemental Composition (%) of Gamma-Ray Sterilized CLPE and CLPE-*g*-MPC

Sample (Sterilization Method)	Surface Elemental Composition (%) (n = 5)			
	C	O	N	P
CLPE (nonsterilized)	99.8 (0.3)[a]	0.2 (0.3)	0.0 (0.0)	0.0 (0.0)
CLPE (25 kGy γ-sterilized)	99.5 (0.2)	0.6 (0.2)	0.0 (0.0)	0.0 (0.0)
CLPE (50 kGy γ-sterilized)	99.1 (0.2)	0.9 (0.2)	0.0 (0.0)	0.0 (0.0)
CLPE-*g*-MPC (nonsterilized)	58.0 (0.2)	31.5 (0.2)	5.2 (0.1)	5.3 (0.1)
CLPE-*g*-MPC (25 kGy γ-sterilized)	63.7 (2.3)	26.0 (2.3)	5.2 (0.1)	5.1 (0.2)
CLPE-*g*-MPC (50 kGy γ-sterilized)	65.0 (0.6)	24.6 (0.5)	5.2 (0.1)	5.2 (0.1)
MPC polymer[b]	57.9	31.6	5.3	5.3

[a] The standard deviation is in parentheses.
[b] Theoretical elemental composition of MPC polymer.

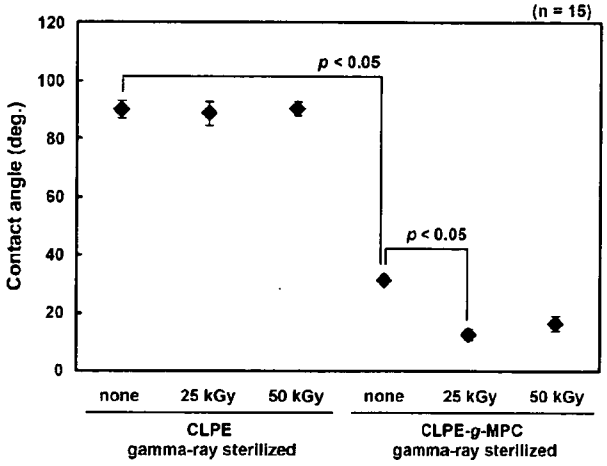

Figure 2. Static water-contact angle of the untreated CLPE and the nonsterilized and the gamma-ray sterilized CLPE-*g*-MPC surfaces. Bar; Standard deviations.

of the untreated CLPE was approximately 90° before and after gamma-ray sterilization, and it drastically decreased (approximately 30°) because of MPC grafting. Furthermore, the static water-contact angles of CLPE-*g*-MPC decreased to 15° after gamma-ray sterilization.

The static and dynamic coefficients of friction of gamma-ray sterilized CLPE and nonsterilized and gamma-ray sterilized CLPE-*g*-MPC are shown in Figures 3 and 4. Both the static and dynamic coefficients of friction of CLPE-*g*-MPC decreased drastically when compared with those of untreated CLPE. The degree of reduction in the coefficient was larger in the latter as compared to the former. Considering the gamma-ray sterilized CLPE-*g*-MPC, regardless of the dose of the gamma-ray sterilization and the cycles, approximately 50% reduction (i.e., 46–65%) was observed in the static coefficients of friction for both the 10 and 100 cycles when compared with those of untreated CLPE. On the other hand, the dose of gamma-ray sterilization affected the dynamic coefficient of friction of CLPE-*g*-MPC. That is, it slightly increased from 0.007 (none) to 0.021 (50 kGy) with an increase in the gamma-ray sterilization dose for 10 cycles. The dynamic coefficient of friction of CLPE-*g*-MPC with gamma-ray sterilization of 50 kGy was 75% greater ($p < 0.05$) than that of CLPE-*g*-MPC with nonsterilization.

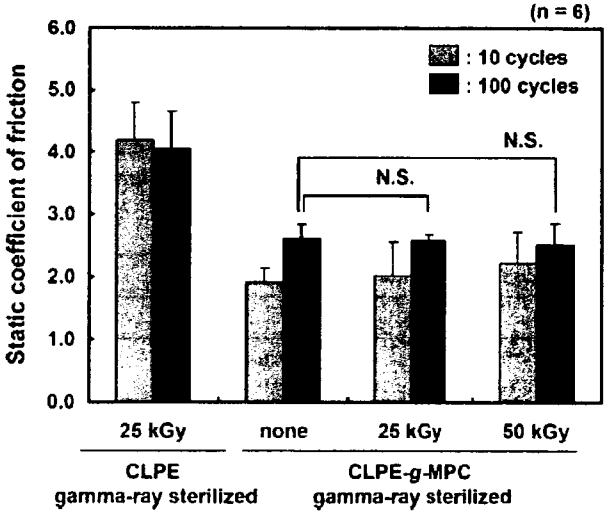

Figure 3. Static coefficients of friction of the gamma-ray sterilized CLPE surfaces and nonsterilized and gamma-ray sterilized CLPE-*g*-MPC surfaces. Bar; Standard deviations.

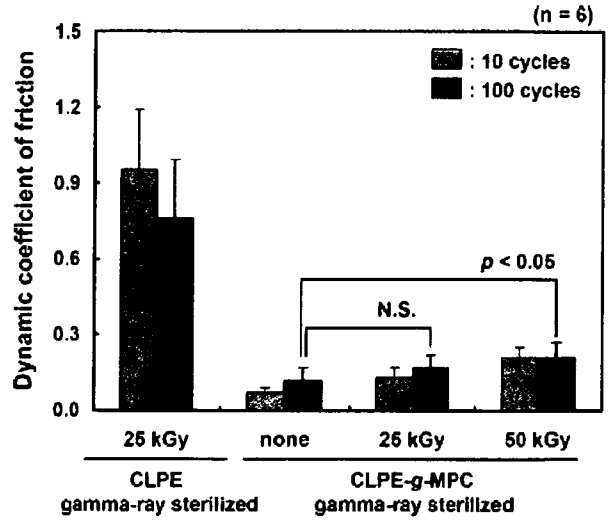

Figure 4. Dynamic coefficients of friction of gamma-ray sterilized CLPE surfaces and nonsterilized and gamma-ray sterilized CLPE-*g*-MPC surfaces. Bar; Standard deviations.

Figure 5 shows the weight change (gravimetric wear) of the gamma-ray sterilized CLPE cups and nonsterilized and gamma-ray sterilized CLPE-*g*-MPC cups in the hip joint simulation test. When the gravimetric method is used, the weight loss was corrected for the fluid absorption by sub-

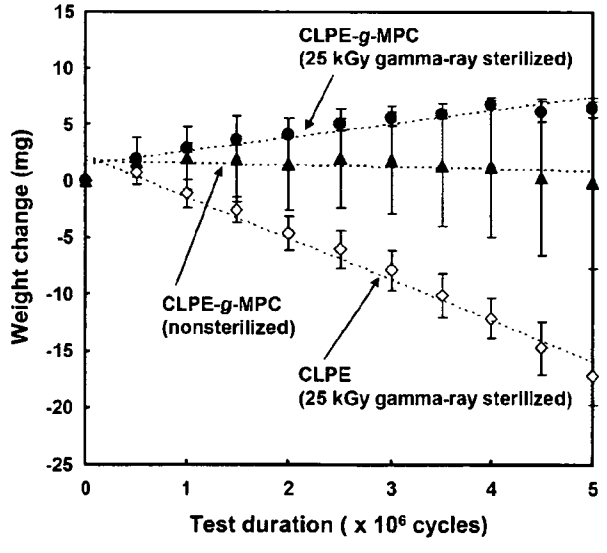

Figure 5. Weight change (gravimetric wear) of gamma-ray sterilized CLPE cups and nonsterilized and gamma-ray sterilized CLPE-*g*-MPC cups in the hip joint simulation test. Bar; Standard deviations.

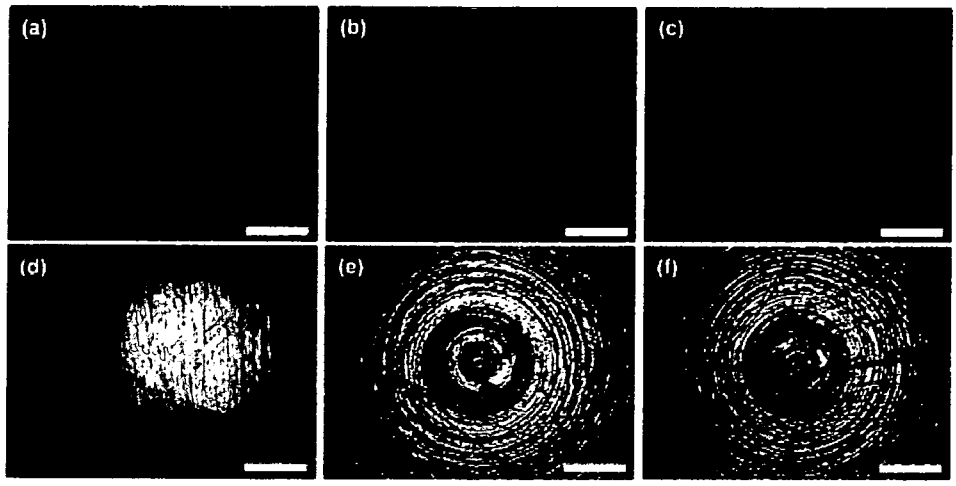

Figure 6. Confocal laser scanning microscope images of the CLPE and CLPE-*g*-MPC bearing surfaces before and after the hip simulator test. (a) CLPE (gamma-ray sterilized), (b) CLPE-*g*-MPC (nonsterilized), (c) CLPE-*g*-MPC (gamma-ray sterilized) before the hip simulator test, (d) CLPE (gamma-ray sterilized), (e) CLPE-*g*-MPC (nonsterilized), and (f) CLPE-*g*-MPC (gamma-ray sterilized) after the hip simulator test. The bar indicates 500 μm.

tracting the weight gain that occurred in the load-soak controls. Since the tested cups are subjected to a motion and load, such a "load-soak" correction is not necessarily satisfactory. Therefore, the tested cups absorb slightly more fluid than their load-soak controls. Consequently, the correction for using the load-soak control data may result in a slight underestimation of the actual weight loss. After 5.0 $\times$ 10^6 cycles of the simulator test, both the CLPE-*g*-MPC cups were found to undergo lesser wear than the untreated CLPE cups. In particular, the gamma-ray sterilized CLPE-*g*-MPC cups showed extremely low and stable wear. As for the nonsterilized CLPE-*g*-MPC cups, the weight change varied for each cup (standard deviation = 7.6 mg, n = 4). Figure 5 indicates that certain gamma-ray sterilized CLPE-*g*-MPC cups exhibit a slight increase in weight because of slightly enhanced fluid absorption when compared with that in the load-soak controls.

Figure 6 shows the confocal laser scanning microscope images of the bearing surfaces of the untreated gamma-ray sterilized CLPE cups and nonsterilized and gamma-ray sterilized CLPE-*g*-MPC cups before and after the simulator test. Before the simulator test, regular circular machining marks were seen on the all the bearing surfaces of the CLPE and CLPE-*g*-MPC cups. After the simulator test, the machining marks on these surfaces of the CLPE cups disappeared completely. On the contrary, clear machining marks with regular circles were observed on the surface of the nonsterilized and gamma-ray sterilized CLPE-*g*-MPC cups, indicating almost no wear on the surface.

DISCUSSION

We have developed an artificial hip joint using CLPE-*g*-MPC on the bearing surface with an objective of reducing wear and avoiding bone resorption. The static and dynamic coefficients of friction of CLPE-*g*-MPC reduced by >50% and >90%, respectively, as compared to those of the untreated CLPE, as shown in Figures 3 and 4. These friction coefficients were much lower than those usually found for the measurable shear interactions between UHMWPE and the Co-Cr-Mo alloy.[29,30] The significant reduction in the coefficients of friction of the grafted MPC polymer resulted in a substantial improvement in wear resistance, as shown in Figure 5. We assumed that the bearing surface of the artificial hip joint combined with the MPC polymer layer 100–200 nm thick exhibited the fluid film lubrication (or mixed lubrication) of the intermediate hydrated layer.[5,7,19]

These sterilizations may affect the properties of medical devices. Generally, when a high energy beam by gamma-ray sterilization is irradiated on a polymer, free radicals are formed by the scission of molecular chains.[20] This is followed by the retermination and cross-linking of the molecules. In this study, we therefore assumed that the extra energy supplied by gamma-ray irradiation produced cross-links in three kinds of regions of the CLPE-*g*-MPC: poly (MPC) layer, CLPE-MPC interface, and CLPE substrate, as shown in Figure 7.

As shown in Table I, the contents of nitrogen and phosphorous in the CLPE-*g*-MPC surface were hardly different between the nonsterilized CLPE-*g*-MPC and the gamma-ray sterilized CLPE-*g*-MPC. On the other hand, the contents of carbon and oxygen of CLPE-*g*-MPC slightly increased and decreased (as a trade-off), respectively, with an increase in the gamma-ray irradiation dose. It was assumed that the energy by gamma-ray irradiation would be used in the scission of C=O in the MPC structure by the degassing of O_2 and subsequently produce cross-links of poly(MPC) with chemical bonding involving C—C.[31,32] The extra energy supplied by gamma-ray sterilization of 25–50 kGy is clearly responsible for producing more cross-links.

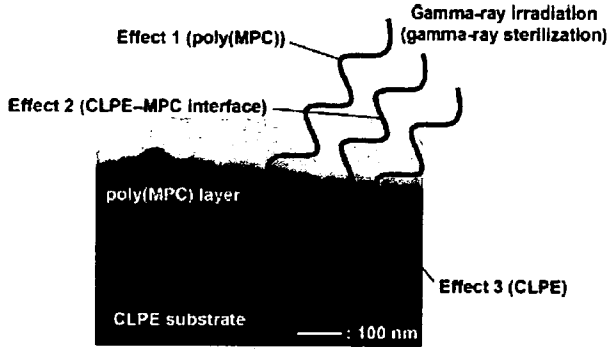

Figure 7. Schematic diagram of the effects of gamma-ray irradiation on CLPE-*g*-MPC.

The dose of gamma-ray sterilization influences the friction response since the dynamic coefficient of friction of CLPE-*g*-MPC slightly increased from 0.007 to 0.021 within the low friction region with an increase in the gamma-ray sterilization dose. It was previously reported that as the polymer concentration (viscosity) increases with the increase in the friction coefficient in the mixed lubrication regime.[33] It was therefore assumed that an ultra-low friction of CLPE-*g*-MPC that appeared during sliding is related to the effective viscosity of poly(MPC) in the mixed lubrication of the intermediate hydrated layer. The viscosity of poly(MPC) reflects the mobility of the free end groups of the MPC polymer or MPC polymer chains themselves; this mobility was limited by the cross-linking of poly(MPC) layer.[34,35] These results seem to suggest that the cross-link corresponds to the viscosity of the poly(MPC) in the bearing interface, the viscosity of the poly(MPC) increases by gamma-ray irradiation, and the poly(MPC) would act as a boundary lubricant in mixed lubrication. These effects are represented as "Effect 1" in Figure 7.

After 5.0×10^6 cycles of the simulator test, the gamma-ray sterilized CLPE-*g*-MPC cups showed low and stable wear (Figure 5). On the contrary, with the nonsterilized CLPE-*g*-MPC cups, the weight change varied in each cup. In the previous study, when a high energy beam was irradiated onto a polymer with a grafted layer, strong bindings were formed between the grafted layer and polymer substrate.[36] Lewis et al. reported that the force required to remove the coating with cross-linking was greater than that without cross-linking.[37] In addition, much more cross-linking and perhaps adhesion to the substrate was induced by the gamma-ray irradiation (gamma-ray sterilization) when compared with the nonsterilized CLPE-*g*-MPC. It is therefore assumed that the higher energy radiation in gamma-ray sterilization induced cross-links not only within the grafting MPC polymer but also between the grafting MPC polymer and CLPE substrate. Then, a much stronger and stable MPC polymer grafted layer was produced on the bearing surface ("Effect 2" in Figure 7).

McKellop et al. reported on the wear performance of UHMWPE in a contemporary hip simulator following gamma-ray irradiation in air as well as in an inert gas and ethylene oxide gas sterilization or gas plasma sterilization.[21] Between 2 and 5×10^6 cycles, the wear rate of the gamma-ray sterilized UHMWPE was significantly lower than that of the UHMWPE sterilized either by gas plasma or ethylene oxide. A similar trend has been reported by Wang et al. who observed more than 50% drop in the hip simulator wear rate after single 25 kGy doses of gamma-ray sterilization.[22] These studies have reported that the wear resistance is better in gamma-ray sterilized UHMWPE than in ethylene oxide sterilized UHMWPE.[21–24] It is therefore assumed that gamma-ray irradiation improved the wear resistance of the CLPE substrate ("Effect 3" in Figure 7).

In the cross-link process of this study, the UHMWPE bar stock was irradiated with a dose of 50 kGy, and then CLPE and CLPE-*g*-MPC were gamma-ray sterilized with a nominal dose of 25 kGy. Thus, the total dosage for the gamma-ray sterilized CLPE and CLPE-*g*-MPC was 75 kGy. The nonsterilized CLPE-*g*-MPC received a total dose of 50 kGy only; this would be a disadvantage for the anti-wear property.[38–40] However, as shown in Figure 6, clear machining marks with regular circles remained on the surfaces of the nonsterilized as well as gamma-ray sterilized CLPE-*g*-MPC cups even after the simulator test. The observed CLPE-*g*-MPC cups were virtually unworn, which is consistent with the relatively low wear in the hip joint simulator tests, as shown in Figure 5. In contrast, the machining marks disappeared from the surface of the gamma-ray sterilized CLPE cups [Figure 6(b)]. In other words, the presence of poly(MPC) on the CLPE surface by MPC grafting would have a greater effect on the wear resistance than the additional cross-links of the CLPE substrate by the gamma-ray irradiation of 25 kGy. The CLPE surface with the poly(MPC) exhibited considerably higher lubricity than that without the poly(MPC) (Figures 2–4). The significant reduction in the coefficient of friction of the grafted poly(MPC) resulted in a substantial improvement in wear resistance. The bearing surface of the artificial hip joint combined with poly(MPC) might exhibit the fluid film lubrication (or mixed lubrication) of the intermediate hydrated layer. This means that artificial hip joints utilizing CLPE-*g*-MPC mimic the natural joint cartilage.[41,42]

The concern about the degradation of polyethylene during shelf aging prompted several orthopedic manufacturers to adopt the sterilization method using gas plasma or ethylene oxide gas for conventional UHMWPE.[43,44] These sterilization methods admittedly generate no free radicals that could be subsequently oxidized during shelf storage. However, UHMWPE sterilized using these methods did not receive the tribological benefit associated with radiation-induced cross-linking. Moreover, the oxidation index of the degraded polyethylene was lower *in vivo* than *in vitro*.[21,45] It has also been reported that the oxygen content might be almost zero in the body.[44,46] Thus, although the oxidation

degradation of polyethylene *in vivo* is related to the surrounding oxygen concentration, that is, that of the body fluid, it is not a main factor of the degradation as a whole. However, recent studies reported that conventional or cross-linked gamma-ray sterilized polyethylene liners undergo *in vivo* oxidation, especially in unworn bearing surface regions and the rim. In contrast, the oxidation of a worn bearing surface was not observed.[47] On the basis of these studies, we assumed that when oxygen is excluded from the package during sterilization, further cross-linking, and additional improvement in the wear performance are attained. However, we must pay attention to the rim fracture in CLPE-*g*-MPC cup by the possible impingements based on the abovementioned studies.[47] In the previous study, for gamma-ray irradiation, the lower molecular weight cross-linked GUR1020 materials had higher mechanical properties (tensile and impact properties) for all doses as compared to the higher molecular weight cross-linked GUR1050 materials.[48] Therefore, we selected a GUR1020 compression-molded bar stock as the CLPE substrate. Nevertheless, the cross-linked GUR1020 materials showed the same wear rate as the cross-linked GUR1050 materials.

Gamma-ray sterilization has had a long history and it has been one of the most popular sterilization methods for various medical products to date. A barrier package has been widely adopted to satisfactorily address the historical problem of the oxidation of gamma-ray sterilized products during shelf storage. In this study, we confirmed that the extra energy supplied by gamma-ray irradiation produced cross-linking in the three regions of the CLPE-*g*-MPC: poly(MPC) layer, CLPE-MPC interface, and CLPE substrate. When the CLPE surface is modified by poly(MPC) grafting, the MPC graft polymer leads to a significant reduction in the sliding friction between the surfaces which are grafted because water thin films formed can act as extremely efficient lubricants. Gamma-ray sterilized CLPE-*g*-MPC showed a slightly higher friction than the nonsterilized one. However, the wear resistance is more stable in the former than in the latter. The cross-links formed by gamma-ray irradiation would give further longevity to CLPE-*g*-MPC cups. Based on the mechanical,[19] biological,[5,49,50] and tribological advantages of MPC polymers, CLPE-*g*-MPC is believed to be promising for use in the next-generation artificial hip joint systems.

The authors also express special thanks to Dr. Masaru Ueno, Mr. Takatoshi Miyashita, and Mr. Noboru Yamawaki (Japan Medical Materials Corp.) for their excellent technical assistance.

REFERENCES

1. Kurtz S, Mowat F, Ong K, Chan N, Lau E, Halpern M. Prevalence of primary and revision total hip and knee arthroplasty in the United States from 1990 through 2002. J Bone Joint Surg Am 2005;87:1487–1497.
2. Harris WH. The problem is osteolysis. Clin Orthop 1995;311: 46–53.
3. Kobayashi A, Freeman MA, Bonfield W, Kadoya Y, Yamac T, Al-Saffar N, Scott G, Revell PA. Number of polyethylene particles and osteolysis in total joint replacements. A quantitative study using a tissue-digestion method. J Bone Joint Surg Br 1997;79:844–848.
4. Sochart DH. Relationship of acetabular wear to osteolysis and loosening in total hip arthroplasty. Clin Orthop 1999;363: 135–150.
5. Moro T, Takatori Y, Ishihara K, Konno T, Takigawa Y, Matsushita T, Chung UI, Nakamura K, Kawaguchi H. Surface grafting of artificial joints with a biocompatible polymer for preventing periprosthetic osteolysis. Nature Mater 2004;3: 829–837.
6. Moro T, Takatori Y, Ishihara K, Nakamura K, Kawaguchi H. Grafting of biocompatible polymer for longevity of artificial hip joints. Clin Orthop Relat Res 2006;453:58–63.
7. Kyomoto M, Moro T, Konno T, Takadama H, Yamawaki N, Kawaguchi H, Takatori Y, Nakamura K, Ishihara K. Enhanced wear resistance of modified cross-linked polyethylene by grafting with poly(2-methacryloyloxyethyl phosphorylcholine). J Biomed Mater Res A 2007;82:10–17.
8. Ishihara K, Ueda T, Nakabayashi N. Preparation of phospholipid polymers and their properties as polymer hydrogel membranes. Polym J 1990;22:355–360.
9. Sawada S, Iwasaki Y, Nakabayashi N, Ishihara K. Stress response of adherent cells on a polymer blend surface composed of a segmented polyurethane and MPC copolymers. J Biomed Mater Res A 2006;79:476–484.
10. Goda T, Konno T, Takai M, Moro T, Ishihara K. Biomimetic phosphorylcholine polymer grafting from polydimethylsiloxane surface using photo-induced polymerization. Biomaterials 2006;27:5151–5160.
11. Sibarani J, Takai M, Ishihara K. Surface modification on microfluidic devices with 2-methacryloyloxyethyl phosphorylcholine polymers for reducing unfavorable protein adsorption. Colloids Surf B Biointerfaces 2007;54:88–93.
12. Ueda H, Watanabe J, Konno T, Takai M, Saito A, Ishihara K. Asymmetrically functional surface properties on biocompatible phospholipid polymer membrane for bioartificial kidney. J Biomed Mater Res A 2006;77:19–27.
13. Bakhai A, Booth J, Delahunty N, Nugara F, Clayton T, McNeill J, Davies SW, Cumberland DC, Stables RH, SV Stent Investigators. The SV stent study: A prospective, multicentre, angiographic evaluation of the BiodivYsio phosphorylcholine coated small vessel stent in small coronary vessels. Int J Cardiol 2005;102:95–102.
14. Watanabe J, Ishihara K. Cell engineering biointerface focusing on cytocompatibility using phospholipid polymer with an isomeric oligo(lactic acid) segment. Biomacromolecules 2005; 6:1797–1802.
15. Abraham S, Brahim S, Ishihara K, Guiseppi-Elie A. Molecularly engineered p(HEMA)-based hydrogels for implant biochip biocompatibility. Biomaterials 2005;26:4767–4778.
16. Konno T, Hasuda H, Ishihara K, Ito Y. Photo-immobilization of a phospholipid polymer for surface modification. Biomaterials 2005;26:1381–1388.
17. Palmer RR, Lewis AL, Kirkwood LC, Rose SF, Lloyd AW, Vick TA, Stratford PW. Biological evaluation and drug delivery application of cationically modified phospholipid polymers. Biomaterials 2004;25:4785–4796.
18. Long SF, Clarke S, Davies MC, Lewis AL, Hanlon GW, Lloyd AW. Controlled biological response on blends of a phosphorylcholine-based copolymer with poly(butyl methacrylate). Biomaterials 2003;24:4115–4121.
19. Kyomoto M, Moro T, Konno T, Takadama H, Kawaguchi H, Takatori Y, Nakamura K, Yamawaki N, Ishihara K. Effects of photo-induced graft polymerization of 2-methacryloyloxyethyl phosphorylcholine on physical properties of cross-linked poly-

ethylene in artificial hip joints. J Mater Sci Mater Med, Forthcoming.
20. Costa L, Luda MP, Trossarelli L, Brach del Prever EM, Crova M, Gallinaro P. Oxidation in orthopaedic UHMWPE sterilized by gamma-ray radiation and ethylene oxide. Biomaterials 1998;19:659–668.
21. McKellop H, Shen FW, Lu B, Campbell P, Salovey R. Effect of sterilization method and other modifications on the wear resistance of acetabular cups made of ultra-high molecular weight polyethylene. A hip-simulator study. J Bone Joint Surg Am 2000;82:1708–1725.
22. Wang A, Sun DC, Yau SS, Edwards B, Sokol M, Essner A, Polineni VK, Stark C, Dumbleton JH. Orientation softening in the deformation and wear of ultra-high molecular weight polyethylene. Wear 1997;203–204:230–241.
23. Digas G, Thanner J, Nivbrant B, Rohrl S, Strom H, Karrholm J. Increase in early polyethylene wear after sterilization with ethylene oxide: Radiostereometric analyses of 201 total hips. Acta Orthop Scand 2003;74:531–541.
24. Manning DW, Chiang PP, Martell JM, Galante JO, Harris WH. In vivo comparative wear study of traditional and highly cross-linked polyethylene in total hip arthroplasty. J Arthroplasty 2005;20:880–886.
25. Ishihara K, Iwasaki Y, Ebihara S, Shindo Y, Nakabayashi N. Photoinduced graft polymerization of 2-methacryloyloxyethyl phosphorylcholine on polyethylene membrane surface for obtaining blood cell adhesion resistance. Colloids Surf B 2000;18:325–335.
26. International Organization for Standardization 15989. Plastics–Film and sheeting–Measurement of water-contact angle of corona-treated films, Geneva, 2004.
27. International Organization for Standardization 14242–1. Implants for surgery–Wear of total hip-joint prostheses–Part 1: Loading and displacement parameters for wear-testing machines and corresponding environmental conditions for test, 2002.
28. International Organization for Standardization 14242–2. Implants for surgery–Wear of total hip-joint prostheses–Part 2: Methods of measurement, 2000.
29. Saikko V. Wear and friction properties of prosthetic joint materials evaluated on a reciprocating pin-on-flat apparatus. Wear 1993;166:169–178.
30. Yao JQ, Laurent MP, Johnson TS, Blanchard CR, Crowninshield RD. The influences of lubricant and material on polymer/CoCr sliding friction. Wear 2003;255:780–784.
31. Bracco P, Brunella V, Luda MP, Brach del Prever EM, Zanetti M, Costa L. Oxidation behaviour in prosthetic UHMWPE components sterilised with high energy radiation in a low-oxygen environment. Polym Degrad Stab 2006;91: 3057–3064.
32. Premnath V, Harris WH, Jasty M, Merrill EW. Gamma sterilization of UHMWPE articular implants: An analysis of the oxidation problem. Ultra high molecular weight poly ethylene. Biomaterials 1996;17:1741–1753.
33. de Vicente J, Stokes JR, Spikes HA. Soft lubrication of model hydrocolloids. Food Hydrocolloids 2006;20:483–491.
34. Raviv U, Frey J, Sak R, Laurat P, Tadmor R, Klein J. Properties and interactions of physigrafted end-functionalized poly (ethylene glycol) layers. Langmuir 2002;18:7482–7495.
35. Raviv U, Glasson S, Kampf N, Gohy JF, Jérôme R, Klein J. Lubrication by charged polymers. Nature 2003;425:163–165.
36. Salleh NG, Glasel HJ, Mehnert R. Development of hard materials by radiation curing technology. Radiat Phys Chem 2002;63:475–479.
37. Lewis AL, Cumming ZL, Goreish HH, Kirkwood LC, Tolhurst LA, Stratford PW. Crosslinkable coatings from phosphorylcholine-based polymers. Biomaterials 2001;22:99–111.
38. McKellop H, Shen FW, Lu B, Campbell P, Salovey R. Development of an extremely wear-resistant ultra high molecular weight polyethylene for total hip replacements. J Orthop Res 1999;17:157–167.
39. Muratoglu OK, Bragdon CR, O'Connor DO, Jasty M, Harris WH. A novel method of crosslinking ultra-high-molecular-weight polyethylene to improve wear, reduce oxidation, and retain mechanical properties. Recipient of the 1999 HAP Paul Award. J Arthroplasty 2001;16:149–160.
40. Oonishi H, Kim SC, Takao Y, Kyomoto M, Iwamoto M, Ueno M. Wear of highly cross-linked polyethylene acetabular cup in Japan. J Arthroplasty 2006;21:944–949.
41. Dowson D, Jin ZM. Micro-elastohydrodynamic lubrication of synovial joints. Eng Med 1986;15:63–65.
42. Williams PF III, Powell GL, LaBerge M. Sliding friction analysis of phosphatidylcholine as a boundary lubricant for articular cartilage. Proc Inst Mech Eng [H] 1993;207:59–66.
43. Willie BM, Ashrafi S, Alajbegovic S, Burnett T, Bloebaum RD. Quantifying the effect of resin type and sterilization method on the degradation of ultrahigh molecular weight polyethylene after 4 years of real-time shelf aging. J Biomed Mater Res A 2004;69:477–489.
44. Kurtz SM, Rimnac CM, Hozack WJ, Turner J, Marcolongo M, Goldberg VM, Kraay MJ, Edidin AA. In vivo degradation of polyethylene liners after gamma-ray sterilization in air. J Bone Joint Surg Am 2005;87:815–823.
45. Kyomoto M, Ueno M, Kim SC, Oonishi H, Oonishi H. Wear of "100 Mrad" cross-linked polyethylene: Effects of packaging after 30 years real-time shelf-aging. J Biomed Sci Polym Edn 2007;18:59–70.
46. Treuhaft PS, McCarty DJ. Synovial fluid pH, lactate, oxygen and carbon dioxide partial pressure in various joint diseases. Arthritis Rheum 1971;14:475–484.
47. Kurtz SM, Hozack W, Turner J, Purtill J, MacDonald D, Sharkey P, Parvizi J, Manley M, Rothman R. Mechanical properties of retrieved highly cross-linked crossfire liners after short-term implantation. J Arthroplasty 2005;20:840–849.
48. Greer KW, King RS, Chan FW. The effects of raw material, irradiation dose, and irradiation source on crosslinking of UHMWPE. In: Kurtz SM, Gsell RA, Martell J, editors. Cross-linked and thermally treated ultra-high molecular weight polyethylene for joint replacements. West Conshohocken: American Society for Testing and Materials; 2003. pp 209–220.
49. Ishihara K, Aragaki R, Ueda T, Watanabe A, Nakabayashi N. Reduced thrombogenicity of polymers having phospholipid polar groups. J Biomed Mater Res 1990;24:1069–1077.
50. Ishihara K, Ziats NP, Tierney BP, Nakabayashi N, Anderson JM. Protein adsorption from human plasma is reduced on phospholipids polymers. J Biomed Mater Res 1991;25:1397–1407.

J Mater Sci: Mater Med (2007) 18:1809–1815
DOI 10.1007/s10856-007-3063-0

Effects of photo-induced graft polymerization of 2-methacryloyloxyethyl phosphorylcholine on physical properties of cross-linked polyethylene in artificial hip joints

Masayuki Kyomoto · Toru Moro · Tomohiro Konno · Hiroaki Takadama · Hiroshi Kawaguchi · Yoshio Takatori · Kozo Nakamura · Noboru Yamawaki · Kazuhiko Ishihara

Received: 15 March 2006 / Accepted: 31 May 2006 / Published online: 5 May 2007

Abstract Osteolysis caused by wear particles from polyethylene in the artificial hip joints is a serious issue. We have used photo-induced radical graft polymerization to graft 2-methacryloyloxyethyl phosphorylcholine (MPC) polymer onto the surface of cross-linked polyethylene (CLPE-*g*-MPC) in order to reduce friction and wear at the bearing surface of the joint. The physical and mechanical properties of CLPE and CLPE-*g*-MPC were not significantly different, expect that the friction coefficient of untreated CLPE cups was 0.0075, compared with 0.0009 for CLPE-*g*-MPC cup, an 88% reduction. After 3.0×10^6 cycles in the hip joint simulator test, we could not observe any wear of CLPE-*g*-MPC cups. We concluded that the advantage of photo-induced radical graft polymerization technique was that the grafted MPC polymer gave a high lubricity only on the surface and has no effect on the bulk properties of the CLPE substrate.

M. Kyomoto (✉) · N. Yamawaki
Research and Development Corporate Division, Japan Medical Materials Corporation, Uemura Nissei Bldg. 9F, 3-3-31 Miyahara, Yodogawa-ku, Osaka 532-0003, Japan
e-mail: kyomotom@jmmc.jp

T. Moro · H. Kawaguchi · Y. Takatori · K. Nakamura
Department of Orthopaedic Surgery, School of Medicine, The University of Tokyo, Tokyo, Japan

T. Konno · K. Ishihara
Department of Materials Engineering, School of Engineering and Center for NanoBio Integration, The University of Tokyo, Tokyo, Japan

H. Takadama
Materials Research and Development Laboratory, Japan Fine Ceramics Center, Atsuta-ku, Nagoya, Japan

Introduction

The most widely used bearing couple for artificial joint systems is the combination of an ultra-high molecular weight polyethylene (UHMWPE) acetabular component and a Co–Cr–Mo alloy femoral component. However, osteolysis caused by wear particles of UHMWPE has emerged as a serious issue [1–3]. Decreasing the number of wear particles from UHMWPE is one way to prevent osteolysis, and different combinations of bearing surfaces and improvements in the bearing materials themselves have been focused. Several highly cross-linked polyethylenes (CLPE) irradiated with 50–105 kGy have been launched since 1998, and they have been used extensively [4]. Gamma-ray and electron beam irradiation at various doses are used by many manufacturers to produce CLPE. In published reports, CLPE produced with 50–105 kGy irradiation shows an 80–90% reduction in wear rate compared with conventional polyethylene [5, 6]. Clinical results have confirmed the excellent anti-wear properties of CLPE. While the efficacy of CLPE is attested by many reports [7–11], the in vivo reduction of wear is only a decrease of 40–60%, so further improvement is desired.

We have recently developed a new-concept artificial hip joint system with 2-methacryloyloxyethyl phosphorylcholine (MPC) polymer grafted onto the surface of CLPE (CLPE-*g*-MPC), aiming to reduce wear and avoid bone resorption [12]. MPC is a methacrylate monomer which has a phospholipid polar group in a side chain, and which is used to make new concept biomaterials as designed by Ishihara et al. [13], who were inspired by the neutral phospholipids of biomembranes. Many polymers consisting MPC unit are widely used as biomaterials [14, 15]. Various medical devices using MPC polymer have already been developed and clinically used with the approval of the

United States Food and Drug Administration. The efficacy of MPC polymer as a biomaterial is well established [15–17].

Based on the biocompatibility and hydrophilicity of MPC polymer, we have been developing new artificial joints with highly lubricated bearing surfaces produced by photo-induced radical graft polymerization. This technique grafts MPC directly to CLPE, forming C–C covalent bonds between the CLPE substrate and the MPC polymer. In this study, we investigated the effects of this photo-induced radical graft polymerization technique on the physical, mechanical and tribological properties of CLPE-*g*-MPC.

Materials and methods

Chemicals and MPC graft polymerization

Benzophenone and acetone were purchased from Wako Pure Chemical Industries, Ltd (Osaka, Japan). MPC was synthesized industrially using the method of Ishihara, et al. [13] and was supplied by AI Bio-Chips Co., Ltd (Tokyo, Japan).

Compression-molded UHMWPE (GUR1020 resin, Poly Hi Solidur Inc., IN, USA) bar stock was gamma-irradiated with 50 kGy in N_2 gas and annealed at 120°C in N_2 gas for cross-linking. The CLPE specimens were machined from this bar stock after cooling. They were immersed for 30 sec in an acetone solution containing 10 mg/mL benzophenone and then dried in the dark to remove acetone at room temperature [18]. The amount of benzophenone adsorbed on the surface was 3.5×10^{-11} mol/cm^2 by ultraviolet spectroscopy according to the previous study [19]. The MPC was dissolved into degassed pure water to a concentration of 0.5 mol/L. CLPE specimens coated with benzophenone were immersed in the aqueous MPC solution. Photo-induced graft polymerization on the CLPE surface was carried out with ultraviolet irradiation of 5 mW/cm^2 for 10 to 360 min at 60°C using a Toshiba D-35 filter to pass only ultraviolet of 350 ± 50 nm wavelength. After the polymerization, the CLPE-*g*-MPC specimens were removed, washed with pure water and ethanol, and dried.

Surface analysis by FT-IR/ATR and XPS

The functional group vibrations of the CLPE and CLPE-*g*-MPC (90 min irradiation) surfaces were examined by Fourier-transform infrared (FT-IR) spectroscopy with attenuated total reflection (ATR) equipment. CLPE and CLPE-*g*-MPC spectra were obtained in 32 scans over the range of 800 to 2000 cm^{-1} with an FT-IR analyzer (FT/IR615, JASCO Co. Ltd., Tokyo, Japan) at a resolution of 4.0 cm^{-1}.

The surface elemental composition of CLPE was analyzed before and after MPC grafting for 90 min by X-ray photoelectron spectroscopy (XPS). The XPS spectra were obtained on an AXIS-HSi165 (KRATOS ANALYTICAL Ltd., UK) equipped with Mg–Kα radiation source biased at 15 kV at the anode. The take-off angle of photoelectrons was kept at 90°.

Surface wettability observation by spray method

The spray method is based on the wetting response of the surface of a cup when exposured to a distilled water mist for a short period [20]. The entire bearing surfaces of CLPE and CLPE-*g*-MPC (23 and 90 min irradiation) cups were uniformly exposed to 15 mL of water mist. The appearance of the cup surfaces was evaluated in terms of wettability within 10 sec after spraying. Ratio of surface area covered by water (water-covered ratio) was determined by using the Win-Roof image processing system (Mitani Corporation Inc., Fukui, Japan).

Evaluation of physical and mechanical properties

The density, swelling ratio, network chain density, molecular weight between cross-links and cross-link density of CLPE and CLPE-*g*-MPC with irradiation for 90 min were evaluated according to the methods previously reported [21]. The CLPE and CLPE-*g*-MPC specimens ($23 \times 23 \times 1$ mm^3) were weighed (approximately 0.5 g, V_1), allowed to swell for 72 h in *p*-xylene containing 0.5 wt% 2-*t*-butyl-4-methylphenol at 130 °C, and were then reweighed (V_2). After reweighing, specimens were immersed in acetone, dried at 60 °C under vacuum, and reweighed (V_3). The swelling ratio, q, was determined from the weight gain and densities of the polyethylene and xylene, and the physical properties were calculated as follows.

(a) Swelling ratio, q

$$q = V_2 / V_3 \tag{1}$$

(b) Network chain density, $v*$

$$v* = ln\,(1 - q^1) + q^1 + \chi q^2 / V_1\,(q^{-2/3} - 0.5q^{-1})$$
$$V_1 = 136\ mL/mol\ ,\ \chi = 0.37\ (polyethylene) \tag{2}$$

(c) Molecular weight between cross-links, M_c

$$M_c = 1 / \bar{M}c = \mathrm{V}v*$$
$$V = 1 / specimen\ density \tag{3}$$